이학박사학위논문

Factors controlling pH in coastal groundwater and seawater of a volcanic island

화산섬 연안 지하수 및 해수 중 pH 의 조절 요인에 관한 연구

2015 년 8 월

서울대학교 대학원
지구환경과학부
이 정 현

Factors controlling pH in coastal groundwater and seawater of a volcanic island

화산섬 연안 지하수 및 해수 중 pH의 조절 요인에 관한 연구

지도교수 김 규 범

이 논문을 이학박사학위논문으로 제출함
2015년 6월

서울대학교 대학원
지구환경과학부
이 정 현

이정현의 박사학위논문을 인준함
2015년 6월

위 원 장 황 점 식 (인)
부 위 원 장 김 규 범 (인)
위 원 신 경 훈 (인)
위 원 박 선 영 (인)
위 원 남 성 현 (인)

Abstract

Factors controlling pH in coastal groundwater and seawater of a volcanic island

Junghyun Lee
School of Earth and Environmental Sciences
The Graduate School
Seoul National University

The oceans are being acidified as a result of oceanic uptake of anthropogenic CO_2, and global surface pH levels have already decreased by more than 0.1 units since preindustrial times. This ocean acidification may have critical consequences for marine ecosystems and biogeochemical cycles. In addition to ocean acidification driven by rising atmospheric CO_2 levels, some coastal regions have experienced more rapid declines in their seawater pH than that in the open ocean as a result of anthropogenic nutrient inputs through river water and groundwater discharge. Although a number of studies have dealt with coastal pH changes related to river water discharge, studies on the effects of coastal groundwater discharge, which has recently been recognized as an important pathway for nutrients, organic matter, and other trace elements, are limited. Therefore, in this study, I aimed to investigate the pH changes in coastal groundwater itself and evaluate the effects of this groundwater discharge on coastal seawater pH.

In order to evaluate pH changes in coastal groundwater, pH (NBS scale),

dissolved inorganic carbon (DIC), total alkalinity (TAlk), and δ^{13}C-DIC were measured in groundwater of a subterranean estuary (STE) in Hwasun Bay, which is located in the southwestern part of Jeju Island that lies off the coast of South Korea. This site was chosen because the amount of submarine groundwater discharge (SGD), which includes a substantial amount of submarine fresh groundwater discharge (SFGD), is large in this area and thus water is exchanged actively between the land and ocean through a sandy sediment layer. In the STE of Hwasun, the pH values (7.4±0.2) of fresh groundwater increased sharply to ~10 and then behaved conservatively in the mixing zone between alkalified fresh groundwater and seawater. Similar patterns were observed for pH at Samyang on the northern coast and at Iho on the northwestern coast of the island. The distributions of DIC, TAlk, δ^{13}C-DIC, Ca^{2+}, and Mg^{2+} in coastal groundwater of Hwasun, along with the results from laboratory experiments on sediment columns, suggest that the increase of pH in this STE is associated with the adsorption of protons (protonation) onto sandy sediments, rather than other geochemical processes. The laboratory experiments that used sediment samples from five different sites (Hwasun, Samyang, Hyeobjae, Hamdeok, and Pyoseon) on Jeju Island showed that the protonation (1) is a common occurrence for various sediments, (2) increases pH effectively for low salinity (salinity <10) groundwater, and (3) depends on the relative amount of transition metal (i.e., Fe, Ti, and Mn) oxides. The chamber experiments at the interface of seawater and groundwater of Hwasun Bay indicate that there is direct seepage of high pH water into the ocean. This increase in pH leads to the corresponding uptake of CO_2 from the atmosphere. Thus, these results suggest that the reaction between groundwater and coastal sediments should be considered as an important driver of pH change that

regulates the magnitude of chemical species in coastal groundwater seeping into the ocean at the volcanic island of Jeju. The effect of protonation of sediments occurs throughout the entire coast of Jeju beach sediments. However, in some STEs where the loading of organic matter is substantial and the residence time of SGD is long enough to allow organic matter to decompose, the decreases in pH down to 7.7 and the increases in DIC up to 2.5 mmol kg^{-1} were observed. Therefore, the pH in coastal groundwater of this volcanic island is controlled mainly by two factors, namely, protonation and organic matter oxidation.

In order to evaluate the effect of SGD on the coastal ocean, variations in pH of coastal seawaters in Hwasun Bay off the volcanic island of Jeju were measured. This bay is situated in the oligotrophic open ocean. In this region, salinities of all coastal waters depend primarily on SGD because of the lack of any contributions from the river or stream waters. A significant increase in pH along the lower-salinity plume zone was observed, and this zone was extended 0.5 km horizontally where it encompassed the waters from the bottom to the surface (<15m water depth). The observed data for the entire bay-water column showed a significant negative correlation (r^2 = 0.82) between salinity and pH. A simple two-endmember (submarine groundwater and offshore seawater) mixing model showed that this pH increase was caused by enhanced biological production, which resulted from the SGD-driven nutrient inputs rather than from the groundwater dilution itself. Since a number of local and regional studies have shown that SGD-driven fluxes of nutrients are comparable to or higher than riverine fluxes, these results from an SGD-dominated environment suggest that SGD may have a significant influence on

coastal biogeochemical changes such as acidification, deoxygenation, and eutrophication.

The change in pH of coastal groundwater discharge and the associated transport of substances (i.e., nutrients, organic matter, and inorganic carbon) may have a great impact on the coastal ecosystem and biogeochemistry of volcanic islands standing in oligotrophic ocean, which is very vulnerable to ongoing acidification. Therefore, the results presented here provides a good starting point for investigating the various effect of SGD on coastal ocean acidification over different temporal and spatial scales.

Keywords: Coastal groundwater, Submarine groundwater discharge (SGD), Subterranean estuary (STE), pH in coastal waters, Protonation, Nutrients, Volcanic island, Ocean acidification

***Student number*: 2004-30946**

Table of contents

List of Tables

List of Figures

1. Introduction

1.1. Coastal ocean pH

Significant emissions of anthropogenic CO_2 to the atmosphere have led to decreases in global surface-ocean pH levels by more than 0.1 units on average since the industrial revolution as shown in Fig. 1.1 (Feely et al., 2004; Doney et al., 2009; Feely et al., 2009). This ocean acidification may have critical consequences for marine ecosystems and biogeochemical cycles via the associated changes in carbonate chemistry in seawater organisms (Caldeira and Wickett, 2003; Sabine et al., 2004; Kleypas et al., 2005; Wootton et al., 2008; Doney et al., 2009). Impacts from ocean acidification might be more serious in coastal areas that cover ~ 30% of oceanic primary production, ~80% of oceanic organic matter burial, most of the benthic oceanic $CaCO_3$ production, and ~50% of oceanic $CaCO_3$ deposition (Gattuso et al., 1998; Balch et al., 2005; Borges and Gypens, 2010). However, changes in pH of coastal ecosystems are more variable than in the open ocean because of temporal cycles in biological productions (Wootton et al., 2008), river discharge (Borges and Frankignoulle, 1999; Salisbury et al., 2008), upwelling (Feely et al., 2008), and human influences on coastal regions (Frankignoulle et al., 1996; Borges and Gypens, 2010). The short-term coastal pH variability is far greater than in the open ocean, whereas the long-term pH trends in some coastal regions have been experienced rapider declines or no clear trend; see Fig. 1.2 (Provoost et al., 2010; Wootton and Pfister, 2012; Duarte et al., 2013). These coastal pH fluctuations are primarily caused by variable metabolic rather than atmospheric CO_2 (Wootton et al., 2008), they are necessarily accompanied by changes in other factors such as nutrients and dissolved

oxygen (DO) concentrations (Cai et al., 2011; Waldbusser et al., 2011; Melzner et al., 2013).

As illustrated in Fig. 1.3, the pH in the coastal ocean can be affected (decreased or increased) by various factors, including that the following geological, chemical, and biological processes:

(1) Terrestrial nutrient input changes the pH of coastal waters. Specifically, biological production that is supported by riverine nutrient input results in an increased surface-water pH levels in coastal regions (Cai, 2003; Borges and Gypens, 2010; Guo et al., 2012). The subsequent re-mineralization of the products then often causes a larger decline in pH in subsurface-water in the coastal ocean than in the pelagic ocean (Cai, 2003; Borges and Gypens, 2010; Cai, 2011; Cai et al., 2011).

(2) Increasing inputs of dissolved organic matter from land lowers coastal water pH via enhancements in oceanic respiration. In some highly productive regions (e.g., mangroves, lake lands, and salt marshes), reports have documented the discharge of river water or coastal groundwater with high dissolved organic carbon (DOC) concentrations and low pH is reported to discharge into coastal ocean regions (Cai et al., 2003; Maher et al., 2013).

(3) Temporal and spatial variations in biological production (photosynthesis, respiration, and calcification) change pH. Primary production increases CO_2 uptake and the corresponding pH. Alternatively, increases in phytoplankton blooms might increase the transport of organic carbon to subsurface waters where it could decompose and decrease the pH. This process has results that are similar to those from excessive nutrient inputs.

(4) Upwelling occurs in some coastal regions and this brings low pH water derived from respiration in deeper layers of the ocean to surface (Feely et al., 2008; Feely et al., 2010; Frieder et al., 2012). This upwelled water typically has relatively high nutrient concentrations, low dissolved oxygen concentrations, and low water temperatures.

(5) Acidic precipitations caused by the combustion of fossil fuels and agriculture activity can lower the pH in the coastal ocean (Doney et al., 2007). The input of strong acids (HNO_3 and H_2SO_4) and bases (NH_3) can also alter the alkalinity and inorganic carbon storage.

(6) Temporal and spatial variations in freshwater input change the pH in coastal waters by reducing their buffering capacity (Salisbury et al., 2008). These variations mainly relate to sea level change caused by global climate change.

Among these potential factors that can affect coastal ocean pH, human induced eutrophication caused by excessive inputs of nutrients from land has been the most frequently reported factors leading to severe changes in pH (Borges and Gypens, 2010; Cai et al., 2011; Wootton and Pfister, 2012; Duarte et al., 2013). In river-dominated coastal regions, high biological production supported by riverine nutrient inputs leads to increased surface seawater pH (Borges and Gypens, 2010; Guo et al., 2012). Then, the subsequent re-mineralization in subsurface waters in the coastal ocean often causes a more rapid decline in pH than that in the pelagic ocean (Cai et al., 2003; Borges and Gypens, 2010; Cai, 2011; Cai et al., 2011). Although a number of studies have dealt with pH change due to nutrient inputs from rivers (Cai et al., 2011; Guo et al., 2012), studies on the effects of coastal groundwater discharge,

which has recently been recognized as an important pathway for nutrients (Paytan et al., 2006; Burnett et al., 2007; Deborde et al., 2008; Johnson et al., 2008), are limited.

1.2. Coastal groundwater pH

Coastal groundwater discharge, in other words, submarine groundwater discharge (SGD) is commonly defined as any water (meteoric groundwater, marine groundwater, or a composite of both) that flows through the marginal seabed into the ocean (Church, 1996; Burnett et al., 2003); see Fig. 1.4. A recent study has revealed that global SGD is 3-4 times larger than global river water discharge, and this was accomplished by the use of an inverse model combined with a global compilation of ^{228}Ra observations (Kwon et al., 2014). Since nutrients are often highly enriched in submarine groundwater (Slomp and Van Cappellen, 2004; Moore et al., 2006; Kim et al., 2008a; Santos et al., 2008; Kim et al., 2011), SGD-driven nutrients enhance phytoplankton production (Slomp and Van Cappellen, 2004; Hwang et al., 2005; Basterretxea et al., 2010; Kim et al., 2011) and benthic production (Waska and Kim, 2011). SGD is often enriched with dissolved inorganic carbon (DIC) and has a low pH as the result of the degradation of organic carbon within coastal aquifers (Gagan et al., 2002; Cai et al., 2003; Dorsett et al., 2011; Liu et al., 2012; Atkins et al., 2013; Cyronak et al., 2013; Szymczycha et al., 2013). It has been reported that DIC fluxes derived from SGD are comparable to the DIC loads carried by rivers in highly productive regions (e.g., salt marshes, mangroves, and lakelands) (Cai et al., 2003; Moore et al., 2006; Maher et al., 2013). Even in river-dominated ocean margins, the DIC flux derived from SGD can represent more than 30% of the riverine flux (Liu et al., 2012). In oligotrophic coastal waters, SGD and the associated nutrient loading may lead to different consequences for water pH and DIC. Kim et al. (2011) reported that primary production in oligotrophic coastal waters depends greatly on the SGD-driven nutrients from volcanic islands.

The biogeochemical behaviors in subterranean estuaries (STEs), where there are mixing zones between meteoric groundwater and intruded seawater in coastal aquifers, can modify the pH of natural groundwater (Fig. 1.5). Aerobic decomposition of organic matter decreases pH (increases pCO_2) excessively in the low salinity groundwater, and the subsequent anaerobic degradation (i.e., via sulfate reduction or methane production) increases pH (and alkalinity) across the entire salinity range (Cai et al., 2003; Atkins et al., 2013). In addition, $CaCO_3$ dissolution often appears as increasing pH in low salinity groundwater (Cai et al., 2003; Singurindy et al., 2004; Dorsett et al., 2011). In STEs characterized by organic-poor sandy aquifers, the physicochemical interactions (i.e., proton adsorption onto sediment minerals) between groundwater and sediments can change the pH of waters flowing from aquifers (Stumm and Morgan, 1996).

The amount of chemical constituents (including nutrients and metals) transferred through SGD can be significantly altered by geochemical conditions, especially pH in STEs (Slomp and Van Cappellen, 2004; Spiteri et al., 2006; Root et al., 2009). A result from Waquoit Bay (Cape Cod, Massachusetts) showed that the pH gradient at the mixing zone of freshwater (pH 5.5) and seawater (pH 7.9) near the beach causes a significant accumulation of iron oxide and the subsequent removal of phosphate (Spiteri et al., 2006). In spite of the potential significance of the biogeochemistry that occurs in STEs on changes in coastal groundwater pH, there have been only a few investigations in limited environments (Cai et al., 2003; Dorsett et al., 2011; Atkins et al., 2013; Cyronak et al., 2013), which were organic-rich (e.g.,

salt marshes, mangroves, and lake lands) or carbonate-rich (e.g., karst regions and lagoons) regions.

1.3. Objectives

The objectives of this study are to expand our knowledge of the factors that control coastal groundwater pH and to investigate the influence of groundwater discharge on coastal seawater in the vicinity of the volcanic island of Jeju, Korea, which is significantly dependent on the submarine groundwater system. The specific objectives of this study are as follows:

(1) To examine the distributions of pH along the entire salinity range in coastal groundwater, and further, to investigate the mechanisms that alter the pH within the coastal aquifers. For this purpose, surveys for biogeochemical parameters, such as dissolved inorganic carbon (DIC), total alkalinity (TAlk), carbon isotopes (δ^{13}C-DIC), and major cations (Ca^{2+} and Mg^{2+}), were conducted. In addition, laboratory experiments with coastal sediments for investigating interactions between coastal waters and sediments were conducted to investigate the interactions between coastal waters and sediments;

(2) To examine the distribution of pH in coastal bay seawater where the area is strongly influenced by SGD, and further, to evaluate the effect of SGD on seawater in this bay. This site is ideal for observing the effects of SGD on coastal water pH because the SGD signature is distinctive, the high nutrient loading to the oligotrophic waters is significant, and the site has no sustained rivers or streams (Kim et al., 2003; Kim et al., 2011). In order to estimate the change in seawater pH caused by the SGD, on-shipboard surveys for DIC, TAlk, and nutrients as well as pH were conducted for seawater in this bay.

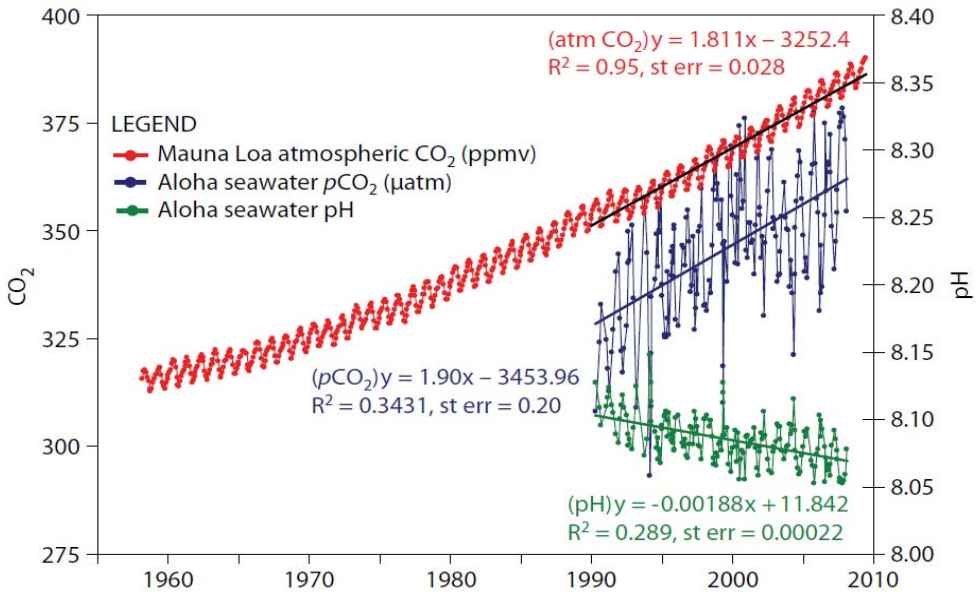

Fig. 1.1. Time series of atmospheric CO_2 at Mauna Loa (ppmv) and surface ocean pH and pCO_2 (µatm) at Ocean Station Aloha in the subtropical North Pacific Ocean (from Feely et al., 2009). The surface ocean pH has already decreased by 0.1 units since the industrial revolution, with the decline rate of 0.0019 units yr^{-1} over the last a few decades.

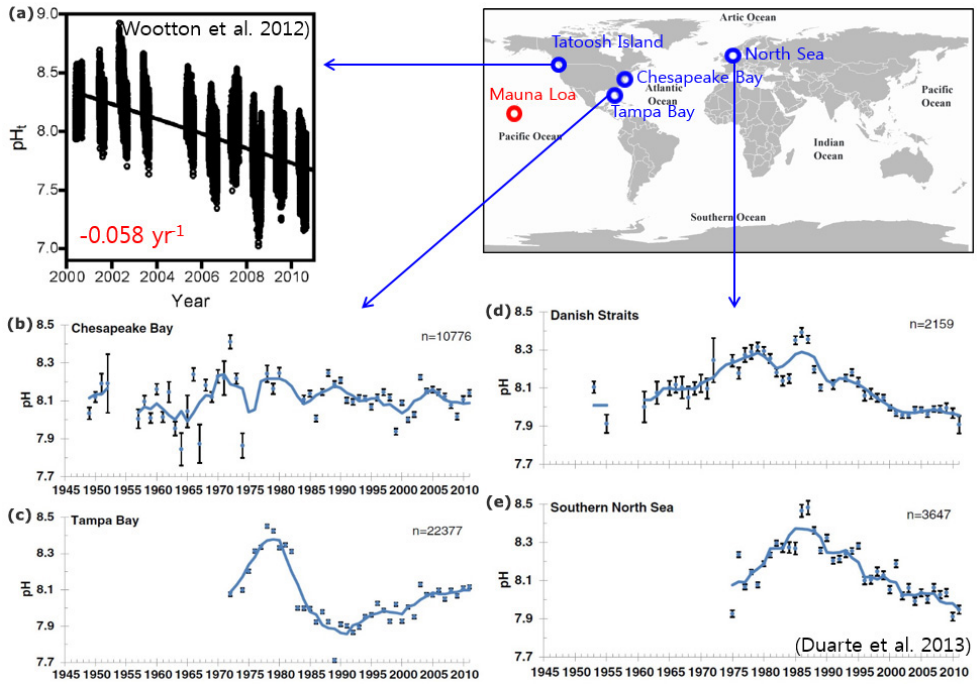

Fig. 1.2. Long-term trends in pH for some coastal regions: (a) Tatoosh Island (from Wootton and Pfister, 2010), (b) Chesapeake Bay, (c) Tampa Bay, (d) Danish Straits in North Sea, and (e) Southern North Sea (from Duarte et al., 2013). The reported long-term trends in surface water pH in coastal ocean reveal a variety of patterns, including periods of both increasing and decreasing pH, which are in response to human alterations of the biogeochemical cycles in coastal ecosystems and their watersheds.

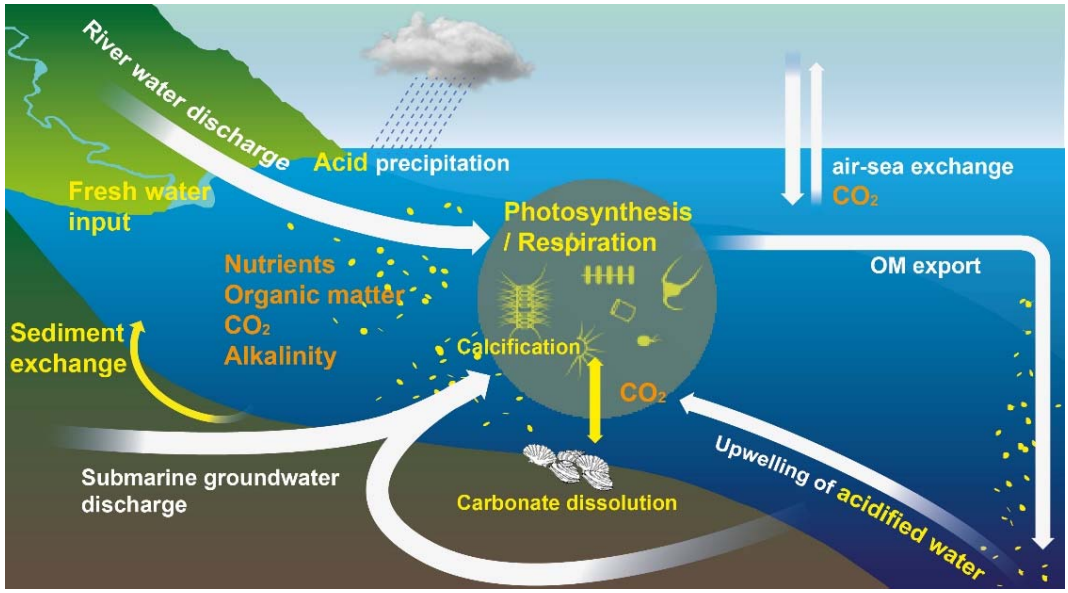

Fig. 1.3. Schematic illustration of various potential factors affecting the pH in coastal ocean: terrestrial input of nutrients and organic matter through river discharge and SGD, spatial and temporal variations of biological production (photosynthesis–respiration, and calcification), upwelling of the acidified water from the deep layer, acid precipitation by human activities, and changes in freshwater input.

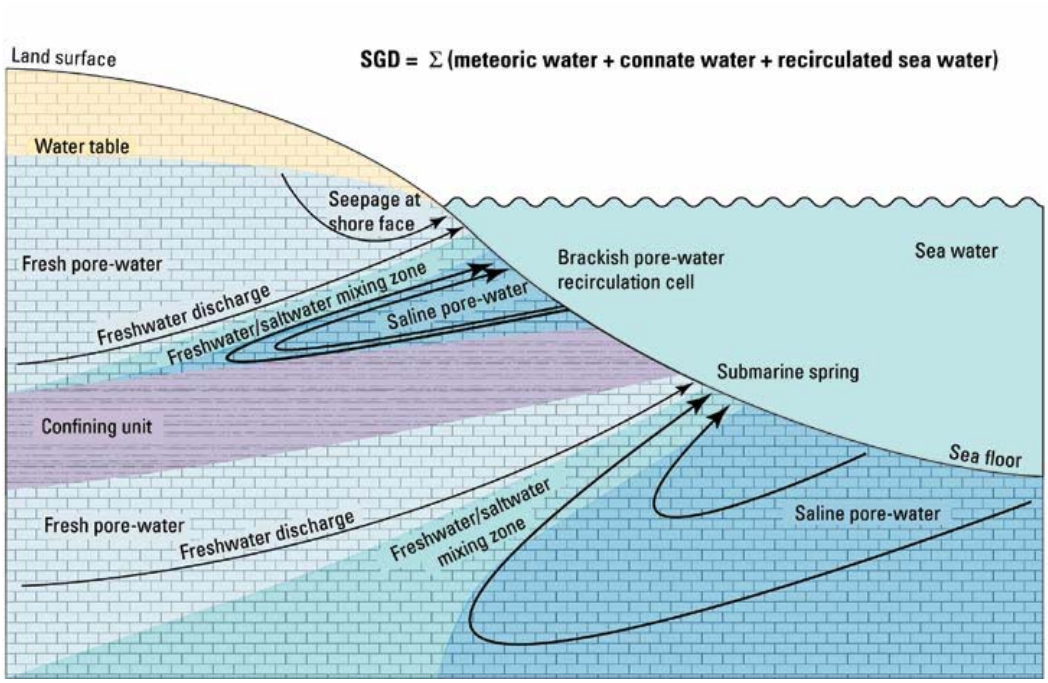

Fig. 1.4. Schematic diagram of an idealized SGD-influenced hydrogeological cross-section (from Kim and Swarzenski, 2010). In this study, SGD is defined as all the direct groundwater outflow across the ocean-land interface (Church, 1996). Thus, SGD includes both the net groundwater discharge and the re-circulated portion of ground-seawater.

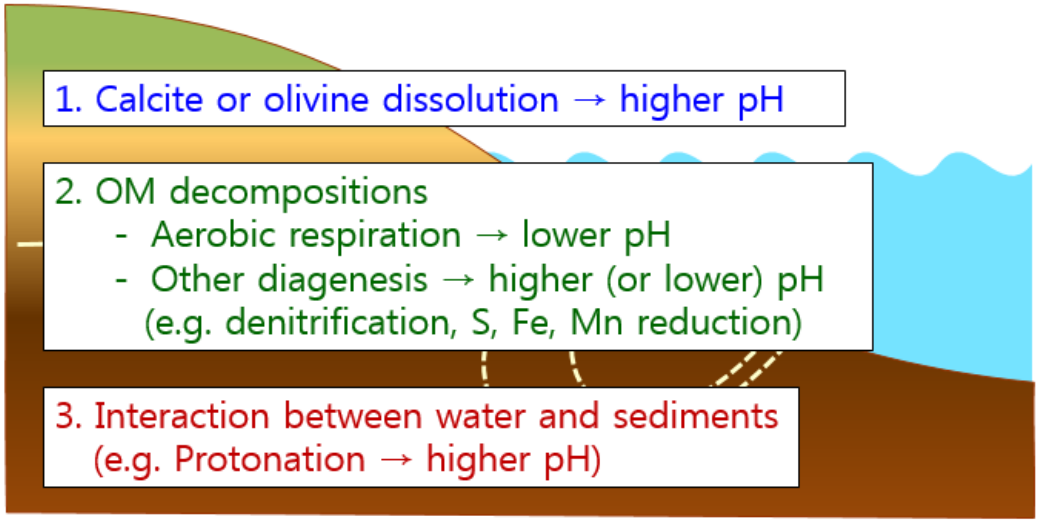

Fig. 1.5. Major biogeochemical reactions which may alter the pH of coastal groundwater in a subterranean estuary (STE).

2. Materials and methods

2.1. Study sites

2.1.1. General features of Jeju Island

Jeju Island is a volcanic island with an area of ~1830 km^2 located in the southern sea of Korea and centered on a shield volcano named Mountain Halla (~ 1950 m elevation). The island lies within the Tsushima Current (salinity >35 and nitrate <1 μM), which originates from the oligotrophic Kuroshio Current (Gong et al., 1996; Ning et al., 1998; Chang et al., 2000).

The island is mainly composed of porous basalt from numerous volcanic eruptions, so Jeju Island has few sustained streams despite high annual rainfall of 1140–1960 mm (Hahn et al., 1997; Koh et al., 2007). Torrents occur only occasionally, after large summer rain events. According to hydrologic budget analyses, almost 50% of total precipitation (1.5×10^9 m^3 yr^{-1}) becomes groundwater recharge (Hahn et al., 1997; Won et al., 2006). The recharged groundwater percolates down through the permeable basaltic rocks and is discharged into the ocean as springs and seepage (Hahn et al., 1997). There are about 383 springs along the coast with a total discharge rate of approximately 3.9×10^8 m^3 yr^{-1} (Hahn et al., 1997). In addition, rapid recirculation of seawater occurs along the coast within the sandy sediments that overlie the thick and highly permeable basaltic layer. Thus, the island's total SGD (Fig. 2.1), including meteoric and marine groundwater, is much larger (~1.5×10^{10} m^3 yr^{-1}; ~300 m yr^{-1}) than that observed for typical continental coasts (Kim et al., 2003; Lee and Kim, 2007).

2.1.2. Hwasun Bay

Abundant meteoric groundwater springs emerge from the deep rocky aquifer at the Hwasun Bay study site located in the southwestern part of Jeju Island. The coastal seawater near Hwasun Bay originates from the Tsushima Warm Current and it is often diluted by Yangtze River diluted water in summer and fall (Lee et al., 2009). The area of the bay is approximately 1.38 km^2. The water is shallow (average 7.6 m, maximum ~15 m depth). The residence time of seawater in this bay, estimated by the tidal prism method (Kim et al., 2011), were approximately 1.3 days.). No sustained stream or river discharges into the bay.

This region has a large amount of SGD (~2.3 × 10^6 m^3 d^{-1}), including substantial submarine fresh groundwater discharge (SFGD) totaling ~5.8 × 10^5 m^3 d^{-1} (Kim et al., 2011). Fresh groundwater springs, from the deep (0–80 m) aquifer (the conductivity 230–340 μS cm^{-1}) through rocks, are ubiquitous and they have uniform geochemical compositions (Won et al., 2005; Won et al., 2006; Koh et al., 2007). In addition, the shallow sandy aquifer (~0.6 m) overlying the basaltic rocks is a very simple system, in which fresh groundwater and seawater become mixed, because of homogeneity of sediment minerals (Kim et al., 2008b), fresh groundwater (Kim et al., 2011; Kim et al., 2013), and coastal seawater. Several sampling campaigns have clearly shown conservative mixing trends for dissolved inorganic nitrogen (DIN), dissolved inorganic silicate (DSi), and dissolved organic carbon (DOC) in this STE (Kim et al., 2011; Kim et al., 2013). Previous studies in this region showed that SGD plays a dominant role in the transport of terrestrial nutrients and

trace elements to the ocean (Hwang et al., 2005; Kim et al., 2011; Kim and Kim, 2011; Jeong et al., 2012).

2.1.3. Other sites in Jeju Island

Jeju Island has a large difference in its geological structures between the western and eastern parts of the island. The Seogwipo formation, which is a low-permeability sedimentary formation, underlies high-permeability basaltic rocks in western Jeju, whereas an unconsolidated fine-sand layer underlies the thick high-permeability volcanic layer in eastern Jeju (Kim et al., 2003). Therefore, there are a number of artesian springs and wells and the associated fresh groundwater seepage on the western coast (e.g. Hwasun, Iho, Samyang), while the SGD is composed almost entirely of recirculated seawater on the eastern coast of Jeju (e.g. Sinyang and Gimnyeong) (Kim et al., 2003). Kim et al. (2003) confirms that recirculated seawater is almost the entire portion of SGD in eastern Jeju, while fresh groundwater contributes to about 20% in western Jeju. Hwang et al. (2005) has shown that Sinyang (Bangdu Bay) often occurs benthic eutrophication owing to large fluxes of excess nutrients from SGD, and that its coastal sediments are usually organic-enriched.

Jeju Island's coastal area are found to be mainly consist of sandy sediments. These sandy sediments were formed by weathering of volcanic rocks consisting of basalt, trachyandesite, tuff, and pyroclastics of advective volcano or biogenic carbonates including shellfish, horny substance of mollusk and keratose of red algae (Kim et al., 2008b). Kim et al. (2008b) classified the coastal areas into three

categories based on their sediment types as silicate sandy beaches (e.g. Samyang), carbonate sandy beaches (e.g. Pyoseon, Gimnyeong, Hamdeok, and Hyebjae), and mixed sandy beaches containing both silicate and carbonate sands (e.g. Hwasun and Iho).

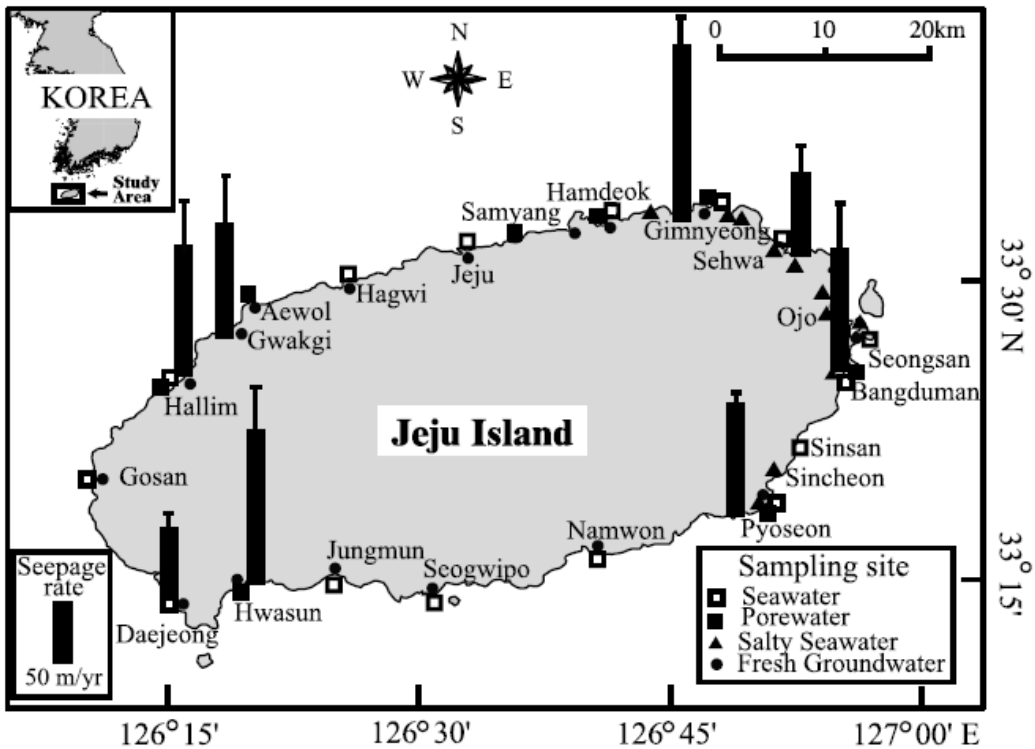

Fig. 2.1. Map of Jeju Island showing submarine groundwater discharge rate (seepage rate) over the entire island (from Kim et al., 2003). The seepage rates measured along the sandy coast were in the range 50–300 m yr^{-1}, which are much higher than those reported from typical continental coast.

2.2. Sampling methods

2.2.1. Coastal groundwater

Hwasun Bay (April and August in 2013)—To obtain data for the coastal groundwater, samples were collected along the shoreline from 22 shallow wells on April 7, 2013 and from 11 shallow wells on August 21, 2013 (Fig. 2.2B). Wells were dug in the sandy aquifer at low tide, to a depth 30–50 cm, where groundwater flows directly into ocean. The shallow wells recharged rapidly enough to collect fresh groundwater within 1–2 minutes. The first fill was discarded, then salinity, temperature, and pH (NBS scale) were measured in situ with a NIST-precalibrated portable multimeter with probes (THERMO Orion Star A329 with 8302BN combination electrode and DuraProbe™ 4-electrode conductivity cells). In addition, two fresh groundwater samples on April 7, 2013 and two samples on August 21, 2013 were collected from a spring flowing from a deep, rocky coastal aquifer (Fig. 2.2). This fresh groundwater springs conducted sampling were clearly visible on the surface. Sampling of coastal groundwater and spring water was limited to beaches on one side of the bay because the other areas are completely rocky. These samples were, however, considered representatives of coastal groundwater for the entire bay because the submarine groundwater in this region has the same water mass as mentioned in chapter 2.1. These samples were taken carefully for the analyses of dissolved inorganic carbon (DIC), total alkalinity (TAlk), δ^{13}C-DIC, major cations (Ca^{2+} and Mg^{2+}), and nutrients as below.

The DIC and TAlk samples were pumped into 500 mL pre-combusted borosilicate bottles poisoned with 200 μL $HgCl_2$ solution and stored with 1%

headspace (Fig. 2.5, Dickson et al. 2007). The δ^{13}C-DIC samples were filtered through a 0.45-μm cellulose acetate membrane (Advantec, 45-mm diameter) into pre-combusted 40 mL vials containing with 20 μL $HgCl_2$ solution and stored without headspace. Samples for major cations (Mg^{2+} and Ca^{2+}) were filtered through a 0.45-μm GF/F membrane (Whatman, 45-mm diameter) into 40 mL vials. All samples were preserved at 4°C. Nutrient samples were collected in 250-mL polyethylene bottles, filtered through pre-combusted 0.7-μm GF/F filters (Whatman, 45-mm diameter) and refrigerated until analysis.

Other sites—In order to compare pH and carbon components in different sandy aquifers of Jeju Island, 13 coastal groundwater samples, with two fresh groundwater samples and two surface seawater samples, were collected in Samyang on August 21, 2013 (Fig. 2.2C). In addition, on September 29–30 in 2014, 15 coastal groundwater samples with two surface seawater samples from Iho, five coastal groundwater samples with two surface seawater samples form Hamdeok, three coastal groundwater samples with two surface seawater samples from Gimnyeong, and six coastal groundwater samples with two surface seawater samples from Sinyang were collected, respectively (Fig. 2.2A). For all samples, salinity, temperature, and pH (NBS scale) were measured in situ with a NIST-precalibrated portable multimeter with probes (THERMO Orion Star A329 with 8302BN combination electrode and DuraProbe™ 4-electrode conductivity cells). Samples for the analyses of DIC were pumped into 24 mL pre-combusted borosilicate vials poisoned with 10 μL $HgCl_2$ solution and stored without headspace (Huang et al., 2012).

2.2.2. Seeping groundwater

Hwasun Bay (August in 2013)—Seeping groundwater samples were taken by a scuba diver from 6 seepage chambers deployed in shallow seawater 1–5 m deep along the shoreline on August 21, 2013 (Fig. 2.2B). The seepage rate was fast enough to collect approximately 3 L of seeping groundwater within 2 hours after the seawater in the chamber was fully replaced. Salinity, temperature, and pH (NBS scale) were measured in situ with a NIST-precalibrated portable multimeter with probes (THERMO Orion Star A329 with 8302BN combination electrode and DuraProbe™ 4-electrode conductivity cells). Samples for the analyses of Talk and DIC were collected into 500 mL pre-combusted borosilicate vials poisoned with 200 μL $HgCl_2$ solution and stored with 1% headspace.

2.2.3. Coastal seawater

Hwasun Bay (April in 2013)—Seawater samples were taken from 11 stations (8 stations inside the bay and 3 stations outside the bay at every 2–3 m of depth; n = 25) in Hwasun Bay over a 4-hour period (from 8:00 a.m. to noon) on April 8, 2013 (Fig. 2.3). The eight stations were selected as the potential points affected by SGD within Hwasun Bay, and the three stations were selected as offshore seawater endmembers. Sampling was conducted onboard a ship by use of a submersible pump with a high-performance conductivity-temperature-depth sensor (Ocean Seven 304, IDRONAUT). At each station, samples were collected for DIC, TAlk, and nutrients, such as dissolved inorganic nitrogen (DIN), dissolved inorganic phosphorus (DIP), and dissolved inorganic silicate (DSi). Samples for DIC and TAlk

analyses were collected in 500-mL glass bottles with 1% of headspace and poisoned with 200 μL of saturated $HgCl_2$ solution following the procedures of Dickson et al. (2007). Nutrient samples were collected in 250-mL polyethylene bottles, filtered through pre-combusted 0.7-μm GF/F filters (Whatman, 45-mm diameter) and refrigerated until analysis.

2.2.4. Sediments for laboratory experiments

For laboratory experiments, sediment samples were taken from five different sites (Hwasun, Pyoseon, Hamdeok, Samyang, and Hyeobjae) in August 19–21, 2013 (Fig. 2.4). Although three subsurface samples (20–50 cm depth) were taken at the upper and lower part of each beach, the results were shown for one sediment sample from each site because the pH increase patterns were almost identical for the samples from the same beach. For example, the pH increase pattern in Hwasun beach was almost the same for 10 samples collected from different sampling depths and locations (surface, subsurface, different locations, different pore-water salinity zones) through in situ pH change experiments (using sediment columns in field). In addition, the X-ray fluorescence (XRF) results (Table 3.9) for one sample from each beach agreed well with those (Table 3.10) from Kim et al. (2008). These sediment samples were refrigerated at -20^{o}C until the pretreatment, analyses, and laboratory experiments.

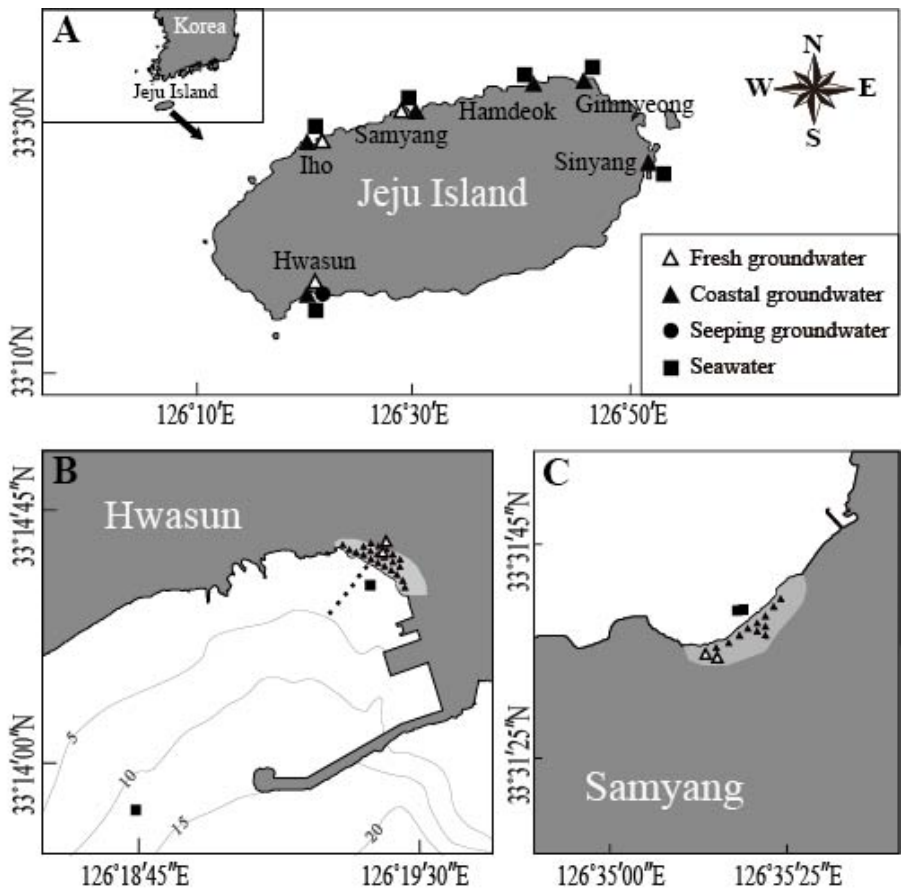

Fig. 2.2. Maps showing sampling locations on Jeju Island, Korea: (A) Six coastal groundwater sampling sites (Hwasun, Iho, Samyang, Hamdeok, Gimnyeong, and Sinyang), three fresh groundwater sampling sites (Hwasun, Iho, and Samyang), one seeping groundwater site (Hwasun), and six surface seawater sampling sites (Hwasun, Iho, Samyang, Hamdeok, Gimnyeong, and Sinyang) for comparison with coastal groundwater; (B) Specific sampling stations for fresh groundwater (open triangles), coastal groundwater (filled triangles), seeping groundwater (circles), and seawater (squares) sampling stations in Hwasun Bay; (C) Specific sampling stations for fresh groundwater (open triangles), coastal groundwater (filled triangles) and seawater (squares) in Samyang.

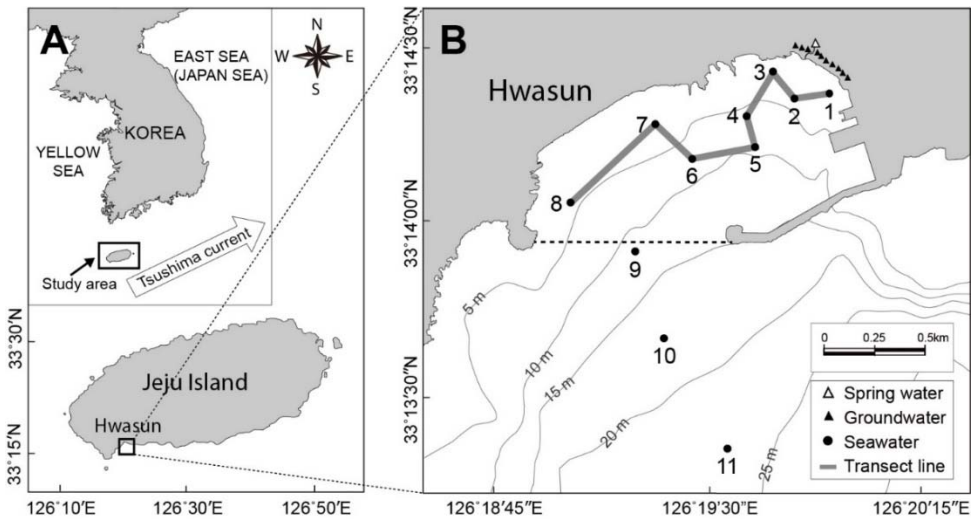

Fig. 2.3. Maps showing the sampling stations on Jeju Island: (A) location of Hwasun Bay; (B) sampling stations of coastal spring water (open triangle), groundwater (filled triangles) and coastal seawater (circles), and a transect line (gray solid line).

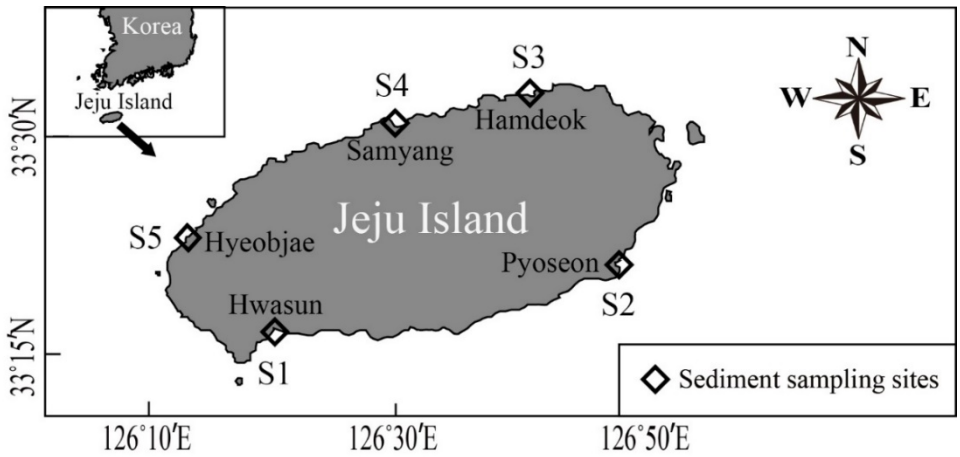

Fig. 2.4. Maps showing sediment sampling locations (Hwasun, Pyoseon, Hamdeok, Samyang, and Hyeobjae) for laboratory sediment column experiments.

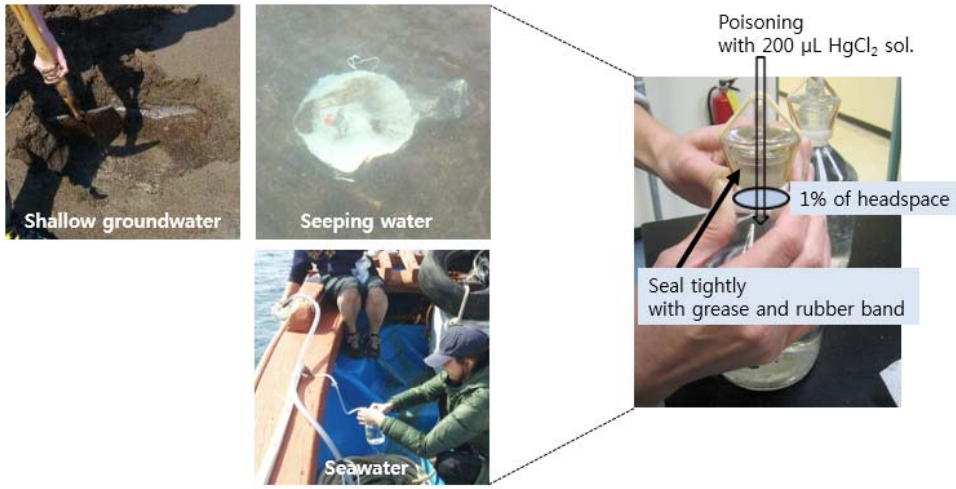

Fig. 2.5. Pictures showing sampling methods of coastal groundwater, seeping groundwater, and seawater for the analyses of DIC and TAlk by use of the VINDTA 3C instrument.

2.3. Analytical methods

2.3.1. Salinity and pH

The salinity and pH (NBS scale) for coastal groundwater were measured in situ with a portable multimeter with probes (THERMO Orion Star A329 with 8302BN combination electrode and DuraProbe™ 4-electrode conductivity cells) that was calibrated against three NBS standards. For coastal groundwater with wide range of pH, the in situ measured pH values has a good correlation ($r^2 = 0.98$, Fig. 2.9) with the pH values calculated from the measured DIC and TAlk by application of the EXCEL macro CO2SYS (Lewis and Wallace, 1998), with constants taken from Mehrbach et al. (1973), as refitted by Dickson and Millero (1987).

The salinity for seawater were in situ measured by use of a high-performance conductivity-temperature-depth sensor (Ocean Seven 304, IDRONAUT). The pH (free scale) for seawater was calculated from the measured DIC and TAlk by application of the EXCEL macro CO2SYS (Lewis and Wallace, 1998), with constants taken from Mehrbach et al. (1973), as refitted by Dickson and Millero (1987). The uncertainties in the calculation of pH from DIC and TAlk (by use of the same method being used here) are known to be <0.01 (Millero, 1995). The free pH scale are used for defining pH in this study because it is more accurate and consistent in seawaters affected by fresh groundwater (Dickson, 1984; Waters and Millero, 2013).

2.3.2. DIC and TAlk

For all samples taken from Hwasun Bay and Samyang, the DIC and TAlk

were measured by use of a Versatile INstrument for the Determination of Total inorganic carbon and titration Alkalinity (VINDTA 3C; Marianda, Germany) coupled to a CO_2 coulometer (Model 5012, UIC Coulometrics), within three weeks after sampling. The VINDTA 3C is a combined system of the standardized alkalinity titration method with a simplified extraction unit for coulometric DIC measurement. The DIC measurement part includes a system for the extraction of CO_2 from a water sample and quantitative transfer of released CO_2 to a coulometric titration unit (Fig. 2.6), and the TAlk part includes a system for titration of a sample with acid and analysis of the titration curve to calculate alkalinity (Fig. 2.7). Sample handling and coulometric titration is controlled by the software. To improve the accuracy of the DIC and TAlk measurements, routine calibration against Certified Reference Material (CRM Batch 128, provided by A.G. Dickson, Scripps Institution of Oceanography) was performed after the analyses of ten samples. The uncertainties for the CRMs were estimated to be 4–6 μmol kg^{-1} (0.3%) for DIC and 1–1.5 μmol kg^{-1} (0.1%) for TAlk during the analyses (Fig. 2.8). In addition, several duplicate sample analyses agreed within these uncertainties.

For samples taken from the other sites (Iho, Hamdeok, Gimnyeong, and Sinyang), the DIC were measured by use of TOC-V_{CPH} analyzer (Shimadzu, Japan); following acidification of 1.0 mL of sample and quantification of the released CO_2 in an infrared detector. Routine calibration against Certified Reference Material (CRM Batch 128, provided by A.G. Dickson, Scripps Institution of Oceanography) was performed after the analyses of ten samples. The uncertainties for the CRMs were estimated to be 10.7 μmol kg^{-1} (0.6%) for DIC. All triplicate sample analyses

agreed within these uncertainties. Although this method has a 2–3 times larger uncertainty than the method using VINDTA 3C, it is advantageous for the DIC analysis of small sample volumes less than 20 mL with a good agreement ($r^2 = 0.99$, Fig. 2.10) with the results from the VINDTA 3C measurement. The TAlk values for these samples were calculated from the measured DIC and pH (NBS scale) by application of the EXCEL macro CO2SYS (Lewis and Wallace, 1998), with constants taken from Mehrbach et al. (1973), as refitted by Dickson and Millero (1987).

2.3.3. δ^{13}C-DIC

The δ^{13}C-DIC samples were analyzed using an isotope ratio mass spectrometer (Isoprime IRMS with a Vario TOC Cube analyzer) following the procedure used by St-Jean (2003). Isotope ratios were determined relative to the international standard Vienna Peedee Belemnite (VPDB). The 10 secondary standard material samples (2mM sucrose) were reproducible within 0.3‰ (Fig. 2.11)

2.2.4. Major cations (Ca^{2+} and Mg^{2+})

The major cation samples were analyzed with an ion chromatography system (Dionex ICS-2100) using a Dionex Ionpac (column: CG16 4 × 250 mm; suppressor: CSRS®300 4 mm). Repeated measurements of standard solutions (prepared from a Dionex stock solution) were reproducible within 2.5% for Ca^{2+} and 3.1% for Mg^{2+} (Fig. 2.12).

2.3.5. Nutrients

Inorganic nutrients were analyzed by use of auto nutrient analyzers (TRAACS 2000-Bran+Lubbe for NH_4^+ and FUTURA PLUS-Alliance for PO_4^{3-}, $Si(OH)_4$, NO_3^-, and NO_2^-) within a week after sampling. In this study, DIN is defined as the sum of NH_4^+, NO_3^-, and NO_2^-, DIP as PO_4^{3-}, and DSi as $Si(OH)_4$. The detection limits of DIN, DIP, and DSi were 0.2, 0.03, and 0.1 μM, respectively, on the basis of three folds of blank values. Uncertainties (standard deviations) were 2.1% for DIN, 2.0% for DIP, and 0.8% for DSi, respectively, for MOOS-1 (23.7 ± 0.9 μM for DIN, 1.56 ± 0.07 μM for DIP, and 26.0 ± 1.0 μM for DSi) from the National Research Council, Canada.

2.3.6. Major elements of sediment samples

Approximately 30 g of each sediment sample was ground to less than 200 mesh using an agate swing mill. Major elements of sediment samples were analyzed at the Research Institute of Advanced Materials, Seoul National University, using an XRF spectrometer (Shimadzu XRF-1800) through the pressed powder pellet method.

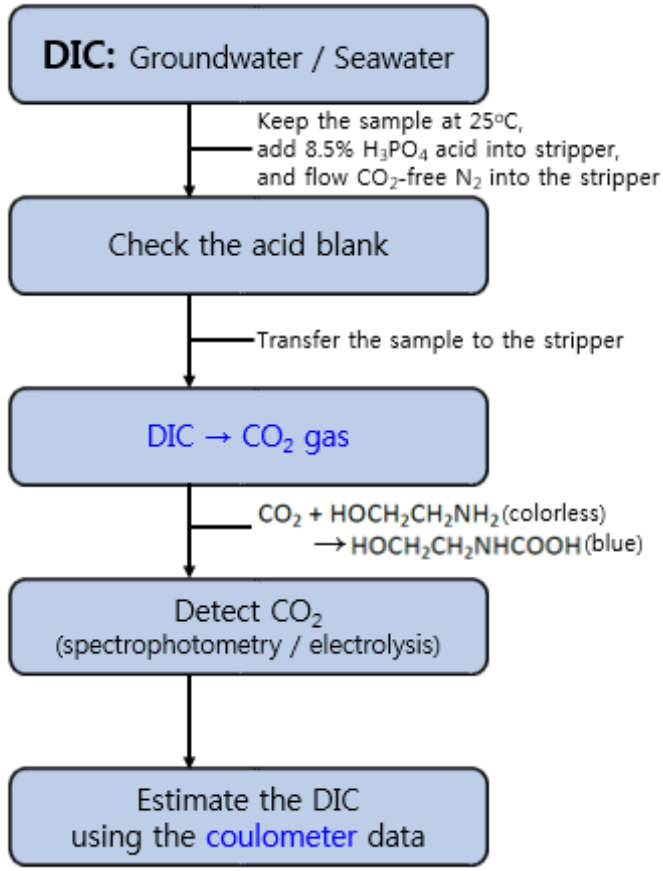

Fig. 2.6. Schematic diagram showing the procedures for measurement of DIC using VINDTA 3C instrument.

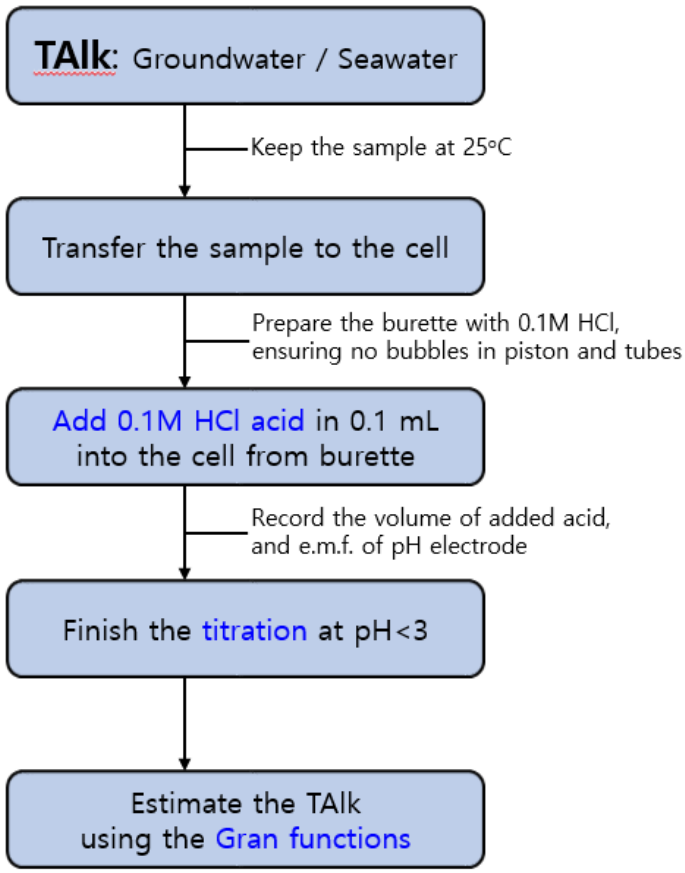

Fig. 2.7. Schematic diagram showing the procedures for measurement of TAlk using VINDTA 3C instrument.

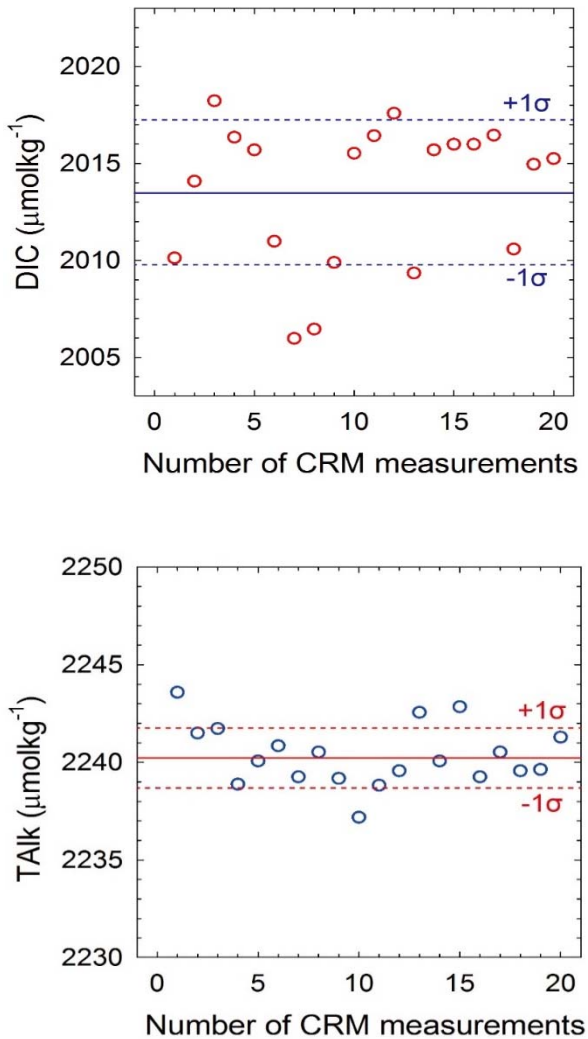

Fig. 2.8. Measured DIC and TAlk concentrations on certified reference materials during the analyses.

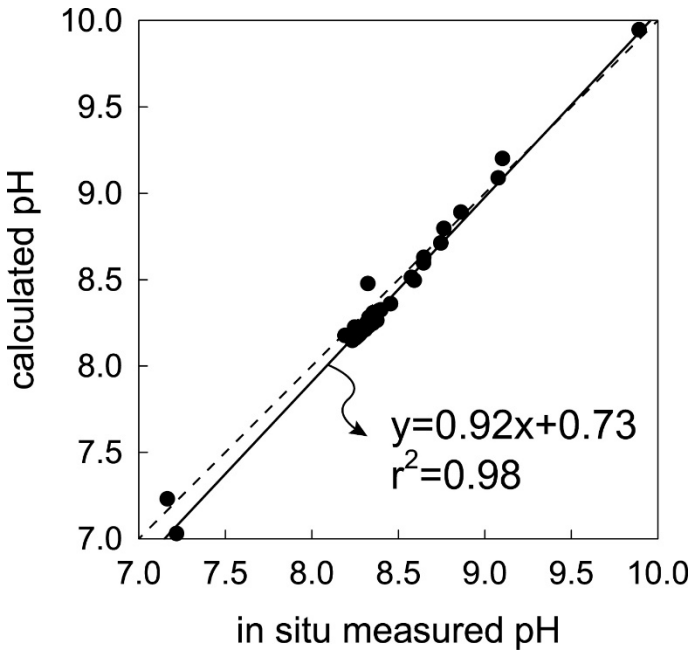

Fig. 2.9. Comparison between in situ measured pH values and calculated pH values from the data of DIC and TAlk (Dataset are obtained from the survey for coastal groundwater conducted in 9 April, 2013).

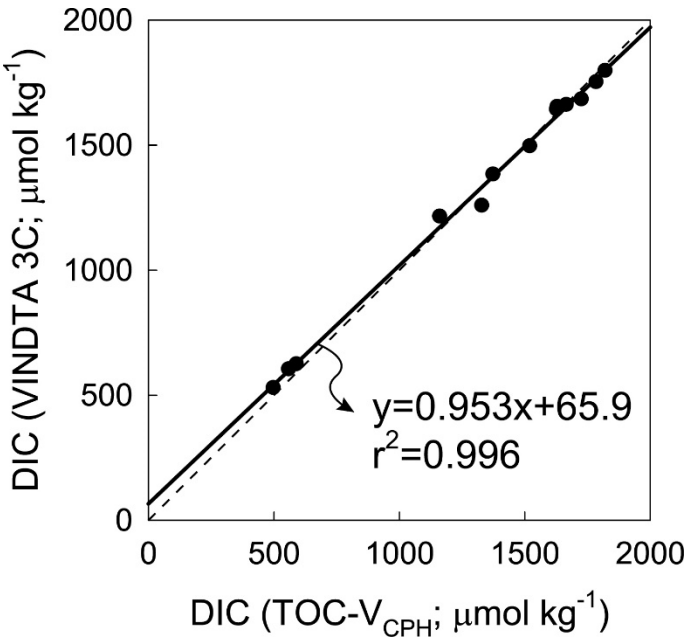

Fig. 2.10. Comparison between the DIC concentrations measured using TOC-V_{CPH} analyzer and those using VINDTA 3C (Samples were collected from the survey for coastal groundwater conducted in 21 August, 2013).

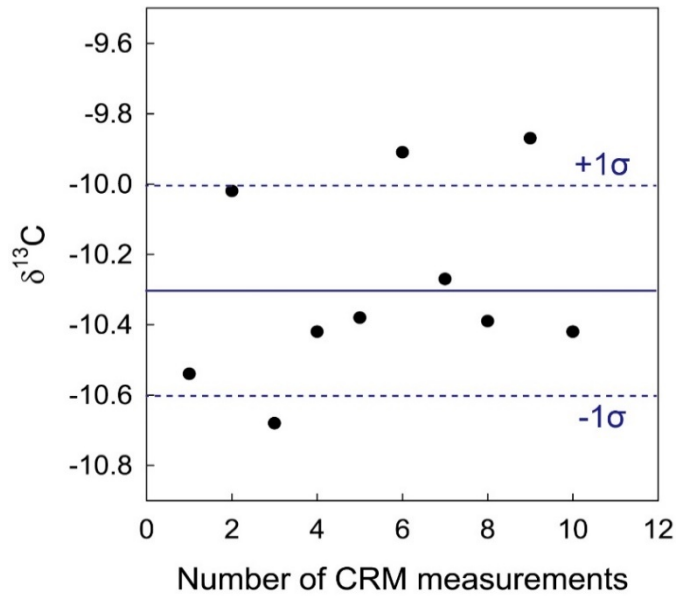

Fig. 2.11. Measured $\delta^{13}C$ on certified reference materials (sucrose 2mM) during the analyses.

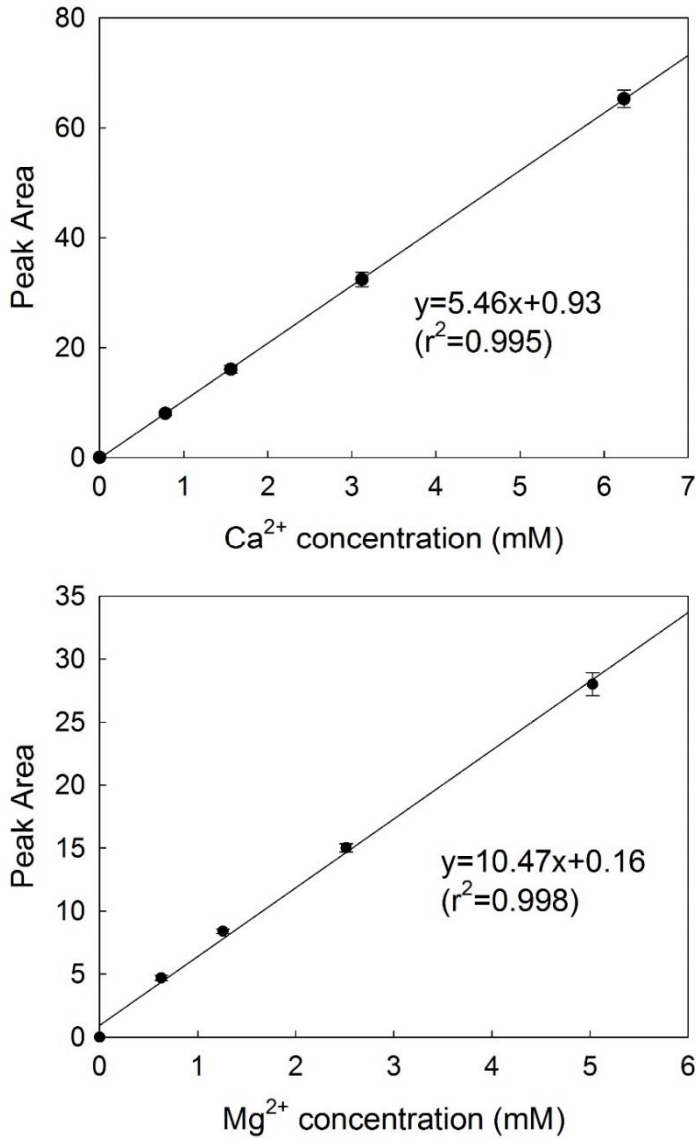

Fig. 2.12. Calibration curve for Ca^{2+} and Mg^{2+} measurements. The error bars represent standard deviations (n=5) for standard solutions.

2.4. Laboratory experiments

2.4.1. Effect of salinity on protonation of sandy sediments

The effect of water salinity on protonation of sediments was examined by flow-through column experiments. Acrylic columns (2.4 cm of inner diameter×25 cm height) were prepared by packing 100 g of Hwasun sediments and sealing one end with sterile poly-gauze to allow only water to pass through the column. Different salinity water samples (salinity 0, 1, 3, 5, 10, 15, 30) were prepared by diluting 0.45 μm filtered seawater with deionized water. Each 2 L sample was fed by gravity through the column. The pH of the effluent collected in a flow-through cell (100-mL) was measured every 30 seconds.

The results from these sediment column experiments will be discussed in chapter 4.1.1.2, specifically.

2.4.2. Protonation extent of various sediments

The effect of sediment type on protonation of sediments was examined by flow-through column experiments for different sediments from 5 sites in Jeju. Using the same column, 1 L of deionized water was passed through each 100 g of sediment samples. The pH of the effluent collected in a flow through cell (100-mL) was measured every 30 seconds. The gravity feeding of 1 L water was completed within 10~40 minutes.

The results from these sediment column experiments will be discussed in chapter 4.1.1.3, specifically.

2.4.3. Long-term capacity of protonation

Long-term capacity of protonation was examined by a flow-through column experiment. A large acrylic column (13 cm of inner diameter×30 cm height) was prepared by packing it with 3.5 kg of dried Hwasun sediments. Tap water was continuously fed through the column (the flow rate was approximately 400 mL min^{-1}) for 50 days. The pH of the effluent collected in a flow-through cell (250 mL) was measured continuously. The pH change was also tested for deionized water with the same procedure for comparison.

The results from these sediment column experiments will be discussed in chapter 4.1.1.2, specifically.

3. Results

3.1. Coastal groundwater

3.1.1. Hwasun Bay

The pH, DIC, TAlk and δ^{13}C-DIC of fresh groundwater as the endmember in Hwasun Bay were 7.4±0.2, 0.58±0.05 mmol kg^{-1}, 0.52±0.05 mmol kg^{-1}, and -9.2±0.8 ‰, respectively. They increased sharply to ~10, ~2.10 mmol kg^{-1}, ~2.63 mmol kg^{-1}, and ~-2.7 ‰, respectively, in the sandy aquifer for coastal groundwater samples, where the salinity is < 1. Then, these components behaved almost conservatively in the fresh groundwater and seawater mixing zone (Table 3.1 and Table 3.2).

3.1.2. Other sites

Similar patterns to the result from Hwasun were observed for pH, DIC, and TAlk at Samyang (Table 3.3), on the northern coast and at Iho (Table 3.4), on the northwestern coast of Jeju Island. The pH, DIC, and TAlk of fresh groundwater as the endmember in Samyang were 7.5±0.1, 0.54±0.05 mmol kg^{-1}, and 0.58±0.07 mmol kg^{-1}, respectively. The pH increased sharply to ~9.4 in the sandy aquifer for coastal groundwater samples, where the salinity is < 1. Then, these components behaved almost conservatively in the fresh groundwater and seawater mixing zone. Although fresh groundwater from coastal springs could not be collected in Iho, the pH values of coastal groundwater in Iho with lower salinity (~8.6) were higher than those of seawater (~8.1) (Table 3.4).

Coastal groundwater in other sites (i.e. Hamdeok, Gimnyeong and Sinyang,

Table 3.5) were mainly consist of recirculated seawater with the salinity range of 32.4–32.8 in Hamdeok, 30.6–32.5 in Gimnyeong, and 27.8–29.9 in Sinyang, respectively. The pH values of coastal groundwater in these regions were relatively lower than the overlying seawater. The pH of coastal groundwater was in the range of 7.7–8.0 in Hamdeok, 7.9–8.0 in Gimnyeong, and 7.7–8.1 in Sinyang, respectively, while the pH of the overlying seawater was in the range of 8.0–8.1 in Hamdeok, 8.4 in Gimnyeong, and 8.2–8.3 in Sinyang, respectively.

3.2. Seeping groundwater (Hwasun Bay)

The salinity, pH, DIC, and TAlk in the seeping groundwater were in the range of 15.6–29.8, 8.1–8.5, 1.46–2.05 mmol kg^{-1}, and 1.74–2.42 mmol kg^{-1}, respectively (Table 3.6). Station 2 represents the zone of mixed SGD with fresh groundwater and marine groundwater.

3.3. Coastal seawater

The coastal groundwater samples taken from the Hwasun Bay beach showed a salinity range of 0.3–33.1. In this subterranean estuary (STE), the pH (free scale) increased sharply from 7.1 to 9.8 at low-salinity sites (salinity <1), and then decreased linearly to the seawater value (pH 8.2) as salinity increased as described in chapter 3.1.1. The DIC and TAlk values were 606–2589 μmol kg^{-1} and 536–2878 μmol kg^{-1}, respectively. The concentrations of DIN, DIP, and DSi were 19–379 μM, 0.7–4.4 μM, and 63–406 μM, respectively. DIN and DSi showed conservative mixing patterns between fresh groundwater and seawater, whereas DIP showed a non-conservative behavior. The data are presented in Table 3.7.

The salinities of seawater in the bay were 34.3–34.6 (mean = 34.5 ± 0.1, n = 22). These values were lower than the salinities of the outer bay, which had a mean of 34.6 ± 0.01 (n = 3). The pH values of seawater in the bay were 8.21–8.31 (mean = 8.25 ± 0.03, n = 21). This value was slightly higher than in the outer bay, which had a mean pH of 8.21 ± 0.01. The concentrations of DIC and TAlk in the bay were 1950–2010 μmol kg^{-1} (mean = 1983 ± 16 μmol kg^{-1}, n = 21) and 2257–2276 μmol kg^{-1} (mean = 2265 ± 5 μmol kg^{-1}, n = 21), respectively. The DIC concentrations within the bay were slightly lower than those in the outer bay (mean = 2010 ± 5 μmol kg^{-1}, n = 3), whereas the TAlk concentrations in the inner and outer bay (mean = 2271 ± 1 μmol kg^{-1}, n = 3) were similar. The concentrations of DIN, DIP, and DSi in the bay were 0.3–1.5 μM (mean = 0.6 ± 0.3 μM, n = 22), 0.02–0.24 μM (mean = 0.12 ± 0.07 μM, n = 22), and 0.3–4.4 μM (mean = 1.1 ± 0.9 μM, n = 20), respectively. The concentrations of DIN and DIP within the bay were similar to those in the outer

bay (mean DIN = 0.7 ± 0.7 μM, n = 3; mean DIP = 0.15 ± 0.09 μM, n = 3), whereas the DSi concentrations within the bay were much lower than those in the outer bay (mean = 2.8 ± 0.2 μM, n=3). The data are presented in Table 3.8.

3.4. Major compositions of sediment samples

According to the XRF results (Table 3.9), sediment samples from Hwasun and Samyang were a mixture of silicate and carbonate sands with high Fe oxide content (9–18 wt. %), whereas samples from Pyoseon, Hamdeok, and Hyeobjae mainly consisted of carbonate sands. These results are agreed well with those (Table 3.10) from Kim et al. (2008).

Table 3.1. Salinity, in situ pH (NBS scale), Concentrations of DIC, TAlk, and concentrations of Ca^{2+} and Mg^{2+} in coastal groundwater (GW), spring water (SP) and offshore seawater for an endmember (SW) in Hwasun Bay observed in 7 April 2013.

Station No.	Salinity	pH	DIC (μmol kg^{-1})	TAlk (μmol kg^{-1})	Cations (mM)	
					Ca^{2+}	Mg^{2+}
GW1	13.8	8.50	1646	1863	2.78	15.8
GW2	15.9	8.49	1653	1883	3.66	18.3
GW3	28.0	8.34	2071	2363	7.47	39.6
GW4	15.5	8.56	2130	2448	3.21	17.6
GW5	5.38	8.99	864.9	1087	2.58	7.72
GW6	19.1	8.69	945.6	1204	7.04	29.4
GW7	23.6	8.32	2877	2589	7.53	40.5
GW8	28.5	8.28	2024	2270	10.3	54.6
GW9	33.1	8.20	1909	2130	10.7	57.6
GW10	23.0	8.29	2256	2484	6.31	35.6
GW11	12.1	8.75	1536	1802	3.98	20.4
GW12	26.1	8.65	1757	2185	8.54	45.3
GW13	19.5	8.46	2524	2815	5.74	32.8
GW14	30.1	8.29	2555	2859	9.48	50.7
GW15	0.58	9.89	1622	2629	0.30	0.48
GW16	3.41	9.08	2104	2549	1.03	4.16
GW17	26.3	8.38	1650	1881	9.24	45.1
GW18	9.74	8.32	1293	1369	3.20	14.9
GW19	3.27	8.86	1843	2106	0.73	3.18
GW20	26.9	8.19	1766	1941	8.46	43.9
GW21	26.1	8.32	1487	1684	8.77	41.8
GW22	26.43	8.35	1666	1895	9.16	46.8
SP1	0.26	7.22	606.1	536.1	0.30	0.39
SP2	0.14	7.16	540.7	471.4	0.27	0.33
SW1	34.58	8.23	2015	2270	9.57	54.7

Table 3.2. Salinity, in situ pH (NBS scale), Concentrations of DIC, TAlk, δ^{13}C-DIC, and concentrations of Ca^{2+} and Mg^{2+} in coastal groundwater (GW) and spring water (SP), and one seawater sample for endmember (SW) in Hwasun Bay observed in 21 August 2013.

Station No.	Salinity	pH	DIC (μmol kg^{-1})	TAlk (μmol kg^{-1})	δ^{13}C-DIC (‰)
GW1	23.7	8.26	1497	1715	
GW2	13.0	8.48	1260	1461	-3.3±0.7
GW3	21.4	8.38	1385	1619	
GW4	8.76	8.95	1216	1576	
GW5	0.15	8.64	605.0	646.6	
GW6	0.36	9.25	1655	2198	-4.9±0.4
GW7	0.65	9.03	2051	2536	-2.7±0.7
GW8	4.35	8.80	1685	1964	
GW9	18.9	8.29	1644	1868	
GW10	13.6	8.45	1663	1903	
GW11	22.2	8.28	1799	2080	-1.7±0.1
SP1	0.14	7.45	624.9	581.4	-8.7±1.1
SP2	0.13	7.58	530.1	506.9	-9.8±1.3
SW1	28.7	8.35	1754	2126	-1.5±0.7

Table 3.3. Salinity, in situ pH (NBS scale), and Concentrations of DIC and TAlk in coastal groundwater (GW) and spring water (SP), and one seawater sample for endmember (SW) in Samyang beach observed in 20 August 2013.

Station No.	Salinity	pH	DIC ($\mu mol\ kg^{-1}$)	TAlk ($\mu mol\ kg^{-1}$)
GW1	5.26	8.95	1305	1644
GW2	2.81	9.24	1291	1744
GW3	4.06	8.91	1065	1298
GW4	9.90	8.70	924.2	1123
GW5	7.99	8.70	1299	1546
GW6	20.4	8.15	1941	2126
GW7	26.1	8.03	1864	2037
GW8	27.2	7.99	1879	2042
GW9	4.15	9.09	1499	1959
GW10	12.1	8.43	1798	1995
GW11	17.3	8.15	1540	1668
GW12	0.21	9.37	755.7	997.7
GW13	0.19	9.17	691.1	870.0
SP1	0.14	7.45	624.9	581.4
SP2	0.13	7.58	530.1	506.9
SW1	26.7	7.90	2051	2189
SW2	28.4	7.88	2018	2153

Table 3.4. Salinity, in situ pH (NBS scale), and Concentrations of (measured) DIC and (calculated) TAlk in coastal groundwater (GW) and two overlying seawater samples (SW) for endmembers in Iho observed in 29 September, 2014.

Station No.	Salinity	pH	DIC ($\mu mol\ kg^{-1}$)	TAlk ($\mu mol\ kg^{-1}$)
GW1	14.8	8.18	2336	2476
GW2	18.5	8.02	2168	2268
GW3	24.8	7.88	2615	2712
GW4	0.69	8.63	1978	2147
GW5	0.99	8.58	1607	1731
GW6	2.89	8.54	2238	2409
GW7	4.58	8.31	2331	2441
GW8	12.8	8.21	2243	2373
GW9	9.90	8.18	1717	1798
GW10	13.3	8.09	2005	2090
GW11	7.84	8.26	1892	1989
GW12	0.43	7.74	1489	1457
GW13	0.45	7.66	1494	1448
GW14	0.57	7.68	1521	1479
GW15	27.4	7.82	1949	2023
SW1	32.1	8.03	1944	2116
SW2	29.8	8.05	1927	2092

Table 3.5. Salinity, in situ pH (NBS scale), and Concentrations of (measured) DIC and (calculated) TAlk in coastal groundwater (GW) and overlying seawater samples (SW) for endmembers in Hamdeok, Gimnyeong, and Sinyang observed in 29 September, 2014.

Station No.	Salinity	pH	DIC ($\mu mol\ kg^{-1}$)	TAlk ($\mu mol\ kg^{-1}$)
Hamdeok				
GW1	32.4	7.77	1952	2029
GW2	32.5	7.74	1942	2010
GW3	32.4	7.95	1946	2086
GW4	32.8	7.90	1964	2088
GW5	32.7	7.94	1925	2062
SW1	32.7	8.05	1863	2043
SW2	32.7	8.10	1869	2072
Gimnyeong				
GW1	30.6	7.94	2090	2223
GW2	32.4	8.07	2028	2225
GW3	32.5	8.03	2173	2360
SW1	32.4	8.37	1924	2293
SW2	32.4	8.37	1938	2309
Sinyang				
GW1	29.5	8.04	1872	2028
GW2	29.3	7.71	2306	2357
GW3	29.2	7.70	2132	2178
GW4	29.9	8.14	1854	2056
GW5	29.9	8.07	1875	2046
GW6	27.8	7.79	2102	2169
SW1	30.0	8.29	1893	2180
SW2	30.1	8.22	1879	2125

Table 3.6. Salinity, in situ pH (NBS scale), and Concentrations of DIC and TAlk in seeping groundwater in Hwasun Bay observed in 21 August 2013.

Station No.	Salinity	pH	DIC ($\mu mol\ kg^{-1}$)	TAlk ($\mu mol\ kg^{-1}$)
1	27.0	8.28	1460	1741
2	15.6	8.48	2055	2416
3	27.6	8.31	1768	2117
4	29.4	8.24	1854	2184
5	29.8	8.19	1876	2183
6	29.8	8.12	1906	2174

Table 3.7. Concentrations of DIC, TAlk, calculated pH (free scale), and nutrients in coastal groundwater (GW) and spring water (SP) in Hwasun Bay observed in 7 April 2013.

Station No.	Salinity	DIC* ($\mu mol\ kg^{-1}$)	TAlk* ($\mu mol\ kg^{-1}$)	pH	Nutrients (μM)			DIN:DIP
					DIN	DIP	DSi	
GW1	13.8	1646	1863	8.50	208	0.67	150	310
GW2	15.9	1653	1883	8.49	232	1.0	128	230
GW3	28.0	2071	2363	8.34	50.5	2.6	97.3	19
GW4	15.5	2130	2448	8.56	239	4.4	107	54
GW5	5.38	864.9	1087	8.99	306	1.9	322	160
GW6	19.1	945.6	1204	8.69	141	2.2	225	63
GW7	23.6	2877	2589	8.32	63.5	0.90	77.8	71
GW8	28.5	2024	2270	8.28	54.9	0.94	69.9	59
GW9	33.1	1909	2130	8.20	19.0	0.90	62.6	21
GW10	23.0	2256	2484	8.29	121	0.94	94.0	130
SP1	0.26	606.2	536.1	7.07	377	2.3	406	160

*The data are from Table 3.1.

Table 3.8. Concentrations of DIC, TA, calculated pH (free scale), and concentrations of nutrients in seawater in Hwasun Bay observed in 8 April 2013.

Station No.	Sampling depth (m)	Salinity	DIC ($\mu mol\ kg^{-1}$)	TA ($\mu mol\ kg^{-1}$)	pH	Nutrients (μM)			DIN:DIP
						DIN	DIP	DSi	
1	0.45	34.47	1976	2262	8.26	0.9	0.14	0.1	6.2
	2.66	34.37	1970	2257	8.26	0.9	0.16	1.7	5.2
2	0.93	34.39	1984	2259	8.25	0.7	0.0	0.0	-
	5.42	34.50	1991	2264	8.24	0.6	0.0	0.4	-
3	0.54	34.49	1979	2262	8.25	1.1	0.18	n.a.	6.2
	2.29	34.48	1977	2262	8.26	0.5	0.16	0.1	3.4
4	0.51	34.41	1982	2262	8.25	0.8	0.0	1.2	-
	2.68	34.44	1978	2264	8.26	0.4	0.0	0.1	-
	6.66	34.48	1993	2263	8.23	4.3	0.0	0.6	-
5	0.42	34.32	1961	2262	8.29	1.0	0.18	0.4	5.6
	3.34	34.33	1967	2264	8.28	0.5	0.29	0.6	1.9
	7.36	34.33	1965	2265	8.29	0.8	0.23	n.a.	3.4
6	0.53	34.58	1995	2270	8.24	0.3	0.05	1.6	6.2
	2.77	34.43	1978	2266	8.27	0.3	0.08	1.3	3.5
	6.29	34.45	1978	2264	8.27	0.3	0.07	0.1	4.1
	9.72	34.32	1950	2260	8.31	0.4	0.07	1.5	5.5

Continued from the previous page

Station No.	Sampling depth (m)	Salinity	DIC (μmol kg^{-1})	TA (μmol kg^{-1})	pH	Nutrients (μM)			DIN:DIP
						DIN	DIP	DSi	
7	0.50	34.60	2002	2272	8.22	0.9	0.15	2.1	6.2
	2.44	34.60	2010	2273	8.21	0.6	0.15	2.0	3.8
	4.48	34.60	n.a.	n.a.	n.a.	0.7	0.16	2.3	4.0
8	0.61	34.55	2003	2270	8.22	0.5	0.17	4.4	2.7
	2.39	34.59	2002	2273	8.23	0.6	0.14	2.5	4.4
	5.37	34.56	2000	2276	8.24	0.4	0.15	2.3	2.8
9	0.73	34.59	2005	2271	8.22	0.2	0.07	2.7	3.0
10	0.49	34.59	2011	2272	8.21	0.5	0.15	2.8	3.2
11	0.73	34.58	2015	2270	8.19	1.5	0.24	3.0	6.2

Table 3.9. Major chemical compositions of sediment samples from Jeju.

No.	Stations	Major chemical compositions of sediments (wt.%)								
		SiO_2	CaO	Al_2O_3	Fe_2O_3	MgO	K_2O	Na_2O	TiO_2	MnO
S1	Hwasun	29.8	20.0	13.4	18.6	13.3	0.655	1.04	2.73	0.194
S2	Pyoseon	5.10	82.5	2.16	2.67	5.92	0.167	0.779	0.493	0.057
S3	Hamdeok	1.63	87.7	0.654	1.00	7.82	0.076	0.669	0.167	0.041
S4	Samyang	43.1	17.9	17.7	9.04	3.81	2.31	3.16	2.26	0.135
S5	Hyeobjae	2.58	89.2	0.949	0.971	5.15	0.101	0.663	0.218	0.026

Table. 3.10. Major chemical compositions of coastal sediments around Jeju (from Kim et al., 2008).

Locations	SiO_2	Al_2O_3	TiO_2	Fe_2O_3	MgO	CaO	NaO	LOI	Etc.	Total
Samyang	49.48	15.74	2.06	10.76	5.65	8.16	3.20	2.32	2.07	99.43
Hamdoek	3.18	0.68	0.13	0.68	3.42	45.39	0.39	41.93	0.40	96.74
Gimnyeong(S)	1.41	–	0.04	0.19	3.44	48.08	0.87	44.39	0.22	98.64
Gimnyeong(L)	6.74	2.35	0.29	1.96	2.56	49.72	0.64	34.26	0.76	99.28
Woljeong	1.78	–	0.05	0.46	2.94	48.18	0.80	43.84	0.24	98.29
Haengwon	4.52	0.63	0.10	1.27	2.90	54.10	0.53	36.11	0.24	100.40
Handong	1.86	0.62	0.08	0.85	2.37	56.42	0.50	37.27	0.24	100.21
Jongdol	14.51	2.42	0.37	5.98	10.71	35.55	0.74	30.29	0.36	100.93
Hongjodangwi	0.28	0.02	–	0.08	5.93	53.13	0.85	39.85	0.10	100.25
Hagosudong	8.13	1.05	0.10	1.03	2.15	51.26	0.99	34.37	0.39	99.47
Gummulae	37.77	8.14	1.79	16.59	15.05	11.23	2.23	6.28	1.11	100.19
SeongSan	36.82	7.15	1.62	18.87	18.81	8.49	1.96	5.33	0.88	99.92
Sinyang	26.00	2.12	0.49	13.48	23.73	16.98	0.33	13.01	0.29	96.46
Pyoseon	3.38	0.45	0.16	0.91	3.20	44.93	0.99	42.00	0.29	96.30
Jungmun	13.67	4.51	0.62	3.04	3.02	37.40	1.36	33.83	0.72	98.17
Hwasun	38.17	9.26	1.14	8.78	8.05	15.52	1.37	17.22	0.86	100.37
Sagye	31.58	5.94	0.66	5.26	6.23	24.97	1.22	22.60	0.96	99.42
Sangmo	49.32	11.02	1.64	11.22	9.13	9.06	2.37	4.82	1.80	100.36
Geumneung	3.92	0.26	0.18	0.83	1.70	48.35	0.67	42.04	0.23	98.18
Hyepjae	1.46	–	0.03	–	3.24	47.97	1.12	49.96	0.23	99.02
Gwidoek	9.41	1.86	0.25	1.79	2.07	49.52	1.57	33.20	0.35	100.02
Gwakgi	3.42	0.59	0.18	0.88	1.82	47.33	1.04	40.68	0.32	96.27
Handam	4.37	0.91	0.11	0.98	1.91	54.38	1.41	35.66	0.20	99.95
Iho	30.55	12.58	0.93	5.15	2.68	23.36	2.86	19.36	1.55	99.04.
Jeju habor	26.16	9.37	0.94	5.01	3.00	27.28	2.46	23.63	1.40	99.27

LOI: Loss of ignition, Unit: wt%.

4. Discussion

4.1. Coastal groundwater

4.1.1. Protonation in Hwasun Bay sediments

4.1.1.1. Change in pH caused by protonation of sandy sediments

The fresh groundwater flowing through the sandy aquifer in Hwasun Bay was instantly alkalified up to pH 10, and then conservatively mixed with marine groundwater (Fig. 4.1). Both DIC and TAlk increased simultaneously (Fig. 4.2). The results from Samyang (Fig. 4.3 and Fig. 4.4) and Iho (Fig. 4.5 and Fig. 4.6) showed a similar increasing pH pattern in the subterranean estuary. The pH of fresh groundwater rose to 9.6 (at Samyang) and 8.7 (at Iho), respectively, and then mixed with seawater in the sandy aquifer (Fig. 4.3 and Fig. 4.5). Corresponding increases in DIC and TAlk were also observed (Fig. 4.4 and Fig. 4.6). These trends suggest that the OH^- production by proton adsorption on sediments rapidly raises pH, DIC, and TAlk as soon as fresh groundwater flows into the sandy layer. The CO_2 in shallow fresh groundwater seems to be in equilibrium with that in air through rapid exchange via sediment pores as illustrated in Fig. 4.18.

The protonation of sediment minerals commonly occurs when sediments react with water (Stumm and Morgan, 1996). This process is formulated as:

$$\text{—}MO^- + H^+ = \text{—}MOH \quad \text{----- (1)}$$

$$\text{—}MOH + H^+ = \text{—}MOH_2^+ \quad \text{----- (2)}$$

where M represents a mineral ion on a surface reactive site. The adsorbed protons can be exchanged by other cations, depending on electrostatic interactions with the substances in the surrounding water. Because the protonation controls the pH of the

water and subsequent acid-base reactions with substances in the water, this process has been investigated mainly as a fundamental mechanism for accumulation or removal of contaminants such as arsenic (Smedley and Kinniburgh, 2002; Arai et al., 2005; Jeong et al., 2010), adsorption or desorption of organic matter (Davis, 1982; Ganor et al., 2009), and precipitation or dissolution of minerals (Casey and Ludwig, 1996; Schott et al., 2009) in aqueous environments.

DIC increase caused by protonation is also supported by the sudden increase in δ^{13}C-DIC values from -9.2±0.8‰ in spring water to -3.8±1.6‰ in the sandy aquifer of Hwasun (Fig. 4.7). The change in carbon isotope ratio can be explained by ^{13}C fractionation caused by CO_2 dissociation for an approximately 4-fold increase in DIC because CO_2 dissociation results in an 8‰–10‰ increase in δ^{13}C-DIC value (Zhang et al., 1995). In addition, it was observed in the field that the pH, DIC, and TAlk of fresh groundwater immediately increased to ~10, 2.41 mmol kg^{-1}, and 3.14 mmol kg^{-1}, repectively, after it flowed through sandy sediment columns (filled with 3.5 kg of sediments) under gravity.

Other effects on the pH involving the oxidation of organic matter, calcite dissolution, and weathering of minerals such as olivine (Mg_2SiO_4) were evaluated using measured δ^{13}C-DIC, Ca^{2+}, and Mg^{2+} data, respectively. As mentioned above, the dissociation of CO_2 was fully responsible for the observed δ^{13}C-DIC values (Fig. 4.7). If there were any inorganic carbon inputs by biodegradation, the values should be lower than the seawater-groundwater mixing line (Boutton, 1991). The effects of calcite dissolution and mineral weathering are also discounted because the

concentrations of Ca^{2+} and Mg^{2+} in this sandy aquifer fall along the salinity mixing line (Fig. 4.8).

4.1.1.2. Effect of salinity on protonation of sandy sediments

The effect of water salinity on protonation of sediments was examined by flow-through column experiments. Acrylic columns (2.4 cm of inner diameter×25 cm height) were prepared by packing 100 g of Hwasun sediments and sealing one end with sterile poly-gauze to allow only water to pass through the column. Different salinity water samples (salinity 0, 1, 3, 5, 10, 15, 30) were prepared by diluting 0.45 μm filtered seawater with deionized water. Each 2 L sample was fed by gravity through the column. The pH of the effluent collected in a flow-through cell (100-mL) was measured every 30 seconds.

The result showed that the pH values of low-salinity water samples (salinity <10) immediately increased from 6.2–7.9 to 8.3–10, while those of high-salinity water samples (salinity>10) remained almost constant at initial values (Fig. 4.9). However, pH increase was reduced as salinity increased, much more than that expected from an increase of buffer capacity, since major cations compete with H^+ for adsorption sites. For high salinity seawater (salinity 30), pH drop at the first stage seemed to be caused by release of H^+ as some cations were exchanged with previously adsorbed H^+. However, high buffer capacity and presence of cations maintained pH of high salinity water back to 8.2. This result is consistent with Mn-impregnated fiber experiments where the pH of deionized water rises to >10 after passing through a Mn fiber column while the pH of seawater drops slightly (Dimova

et al., 2008). Dimova et al. (2008) explained that H^+ competes with cations in seawater or some groundwaters when they adsorb onto the charged sites of sediment surfaces. This is also consistent with the conservative mixing pattern between alkalified fresh groundwater and seawater in the sandy aquifers of the study sites.

4.1.1.3. Protonation extent of various sediments

The effect of sediment type on protonation of sediments was examined by flow-through column experiments for different sediments from 5 sites in Jeju. Using the same column, 1 L of deionized water was passed through each 100 g of sediment samples. The pH of the effluent collected in a flow through cell (100-mL) was measured every 30 seconds. The gravity feeding of 1 L water was completed within 10~40 minutes.

The results show that the pH of deionized water increased from 6.2 to 9.2–10 for all 5 sediment samples (Fig. 4.10). The pH increase was higher for S1 (10) and S4 (9.6) sediment samples than the other samples (9.2–9.4). This difference could be associated with the specific metal oxides (i.e., transition metal oxides) which generally accommodate charged ions in their structure (Kung, 1989). Thus, ΔpH (the pH difference between initial and final pH for the column experiments) was compared for each sediment sample against the metal oxide contents (Fig. 4.11). Specific metal oxides such as Fe, Ti, and Mn correlated well with ΔpH (r^2 >0.8). These results suggest that all sandy sediments occurring at Jeju Island, which contain ferromanganese minerals and mica (e.g., hematite, magnetite, and biotite), are capable of protonation although the extent of protonation may be different for

different locations.

4.1.1.4. Long-term capacity of protonation

Long-term capacity of protonation was examined by a flow-through column experiment. A large acrylic column (13 cm of inner diameter×30 cm height) was prepared by packing it with 3.5 kg of dried Hwasun sediments. Tap water was continuously fed through the column (the flow rate was approximately 400 mL min^{-1}) for 50 days. The pH of the effluent collected in a flow-through cell (250 mL) was measured continuously. The pH change was also tested for deionized water with the same procedure for comparison.

The pH of tap water (river water source) increased immediately up to 10 and then decreased slightly (Fig. 4.12). The pH increased and remained, however, at a relatively lower pH than that of deionized water. The difference was caused by presence of cations competing with H^+. Nevertheless, the pH of tap water maintained a higher pH (8.5) than its initial value (7.6) even after passing more than 30,000 L of tap water through the column for 50 days (Fig. 4D).

This result shows that the capacity of protonation by sandy sediments is strong enough to control the pH in natural waters in the real world over a long period. If this result is extrapolated to the Hwasun beach with a fresh groundwater discharge rate of ~400 m^3 d^{-1} and a sediment amount of ~3×10^7 kg, the lifetime of the protonation capacity could reach 2,000 years. It was also found that the sediments recovered protonation capacity after they were air dried. Since the sand easily

recovers protonation capacity when exposed to air during vertical and horizontal tidal fluctuations, the capacity of protonation by Hwasun sediments seems to be limitless.

4.1.2. Factors controlling pH changes in coastal groundwater at Jeju Island

The pH and salinity from six different sandy aquifers in Jeju Island have wide ranges of 7.6~10 and of 0.1~33, respectively (Table 3.1–Table 3.5). As mentioned in chapter 2.1, the coastal groundwater has large fresh SGD contributions in the western part, while it consists of mostly recirculated seawater in the eastern coast. In the regions occurring large discharge of fresh groundwater, such as Hwasun, Samyang, and Iho, the coastal groundwater with the lower salinity has the higher pH (Fig 4.1, Fig. 4.3, and Fig. 4.5). The pH values in Iho were slightly lower in salty groundwater (salinity >20) than the overlying seawater (Fig. 4.5). The pH values of coastal groundwater in Hamdeok, Gimnyeong, and Sinyang, which is mostly consist of recirculated seawater, were also lower than the overlying seawater (Fig. 4.13). The lower pH values may be result from aerobic oxidation of organic matter. The distributions of the DIC concentrations in Hamdeok, Gimnyeong, and Sinyang were also confirmed this hypothesis with higher values than the overlying seawater (Fig. 4.14).

In order to confirm that organic matter oxidation is the factor lowering pH in this coastal groundwater, two exemplary sediment samples were chosen for monitoring pH variation of seawater incubated in the bottles. A set for the sample from Hwasun, where has organic-poor sands, and the other for the sample from

Sinyang, where has organic-enriched sand. Each sediment sample (approximately 750 g of sediments) was incubated in a 500 mL HDPE bottle filled up with seawater (approximately 160 g of waters) in the dark at 20°C for a month. Replicate bottles were taken at appropriate time intervals (30 minutes to 6 days) for measuring pH and DIC concentrations. Before taking the water samples, the bottles were gently stirred to mix the water overlying the sediments (depths of overlying water were less than 2 cm) and the pore water. There was little variation in the pH and DIC of seawater over the entire incubation time (30 days) for Hwasun sands (Fig.4.16a). In contrast to the result for sand sample from Hwasun, the pH of seawater for the sample from Sinyang substantially had decreased down to 7.7 and the DIC increased from 2.1 mmol kg^{-1} to 2.5 mmol kg^{-1} over the entire time (Fig. 4.16b). This result obviously showed that in situ CO_2 production by organic matter oxidation lowers the pH in the coastal groundwater as the observation in Iho, Hamdeok, Gimnyeong, and Sinyang (Fig. 4.15).

Therefore, I suggest (1) that protonation raises the pH in fresh groundwater flow through the coastal sandy aquifer, and (2) that organic matter oxidation lowers the pH with increasing the residence time of the coastal groundwater in the sediment pores.

4.1.3. pH in seeping groundwater

The discharge of the alkalified groundwater into the ocean was determined by locating 6 seepage chambers on the bottom sediments of Hwasun Bay at water depths of 1 to 5 m (Fig. 2.2B and Fig. 4.17). Although marine groundwater was

dominant for all chamber samples (salinity: 15–30), a significant input of fresh groundwater with high pH occurred at station 2 (salinity: 15.6; pH: 8.5) (Fig. 4.17A, B). At station 2, the concentrations of DIC (~2.1 mmol kg^{-1}) and TAlk (~2.4 mmol kg^{-1}) were also higher than those at the other stations and seawater (Fig. 4.17C, D), as expected from the reaction in the sandy aquifer (Fig. 4.1). This result indicates that the flow of the alkalified water is connected directly to the ocean.

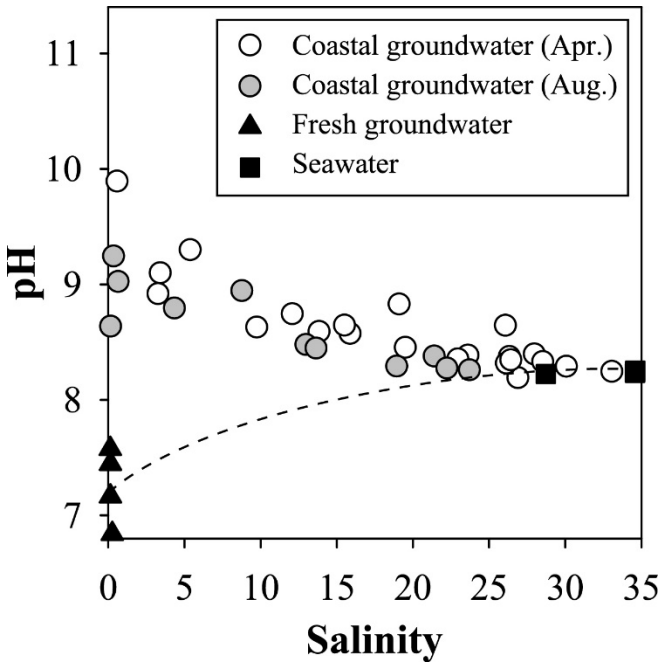

Fig. 4.1. Distributions of pH in coastal groundwater along the salinity gradients at Hwasun Bay. Dotted lines indicate the values expected from conservative mixing between fresh groundwater (triangles) and seawater (squares).

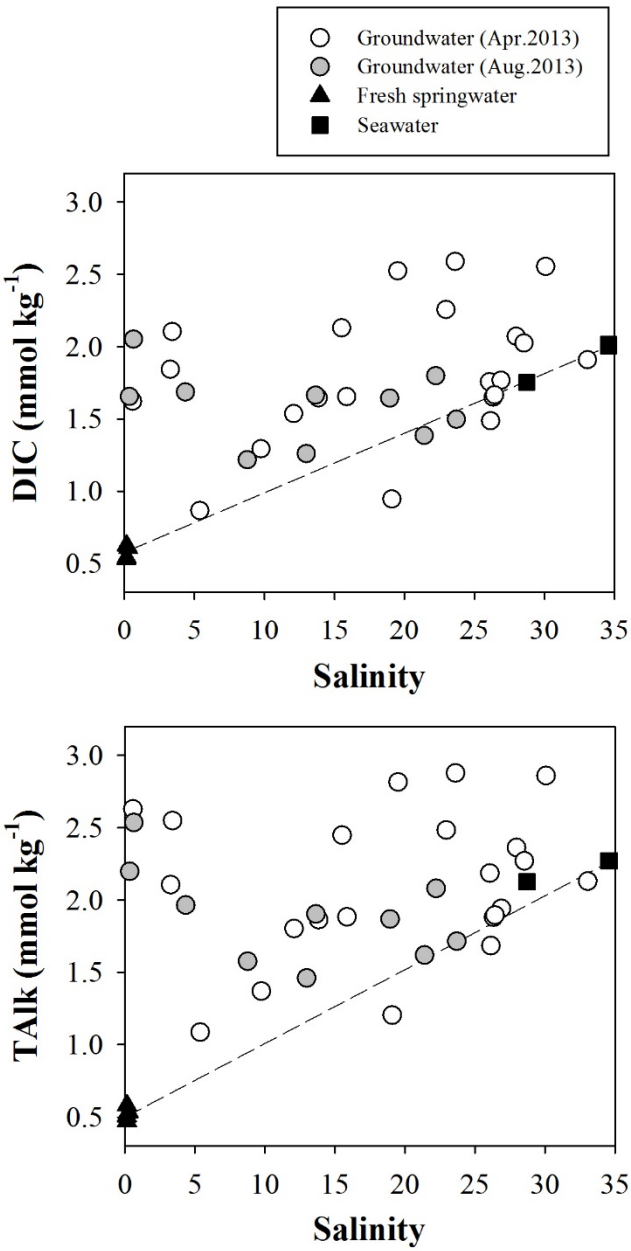

Fig. 4.2. Distributions of DIC and TAlk in coastal groundwater along the salinity gradients at Hwasun Bay. Dotted lines indicate the values expected from conservative mixing between fresh groundwater (triangles) and seawater (squares).

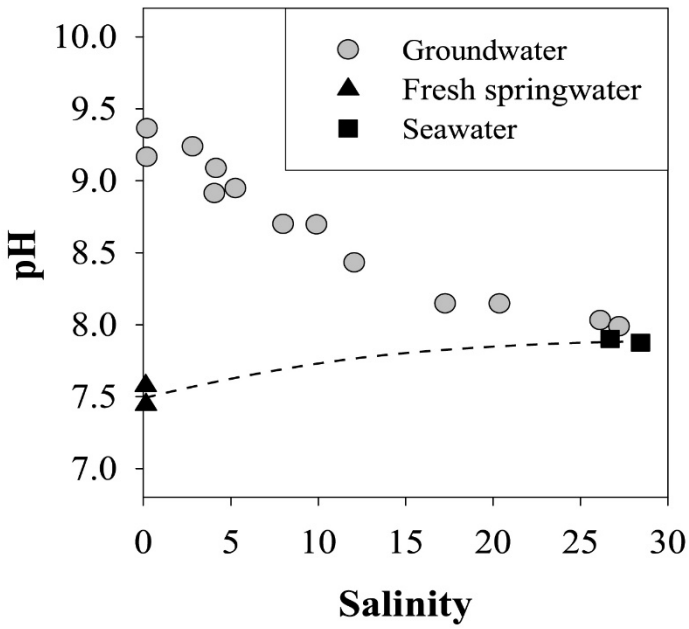

Fig. 4.3. Distributions of pH in coastal groundwater along the salinity gradients at Samyang. Dotted lines indicate the values expected from conservative mixing between fresh groundwater (triangles) and seawater (squares).

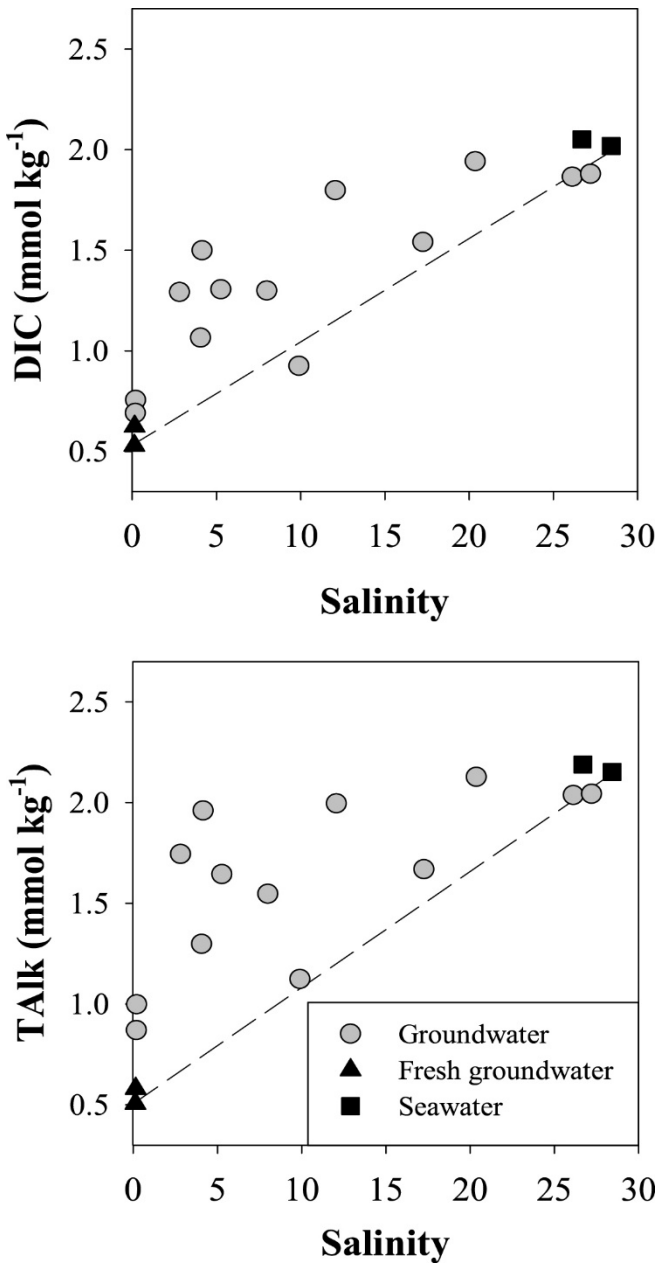

Fig. 4.4. Distributions of DIC and TAlk concentrations in coastal groundwater along the salinity gradients at Samyang. Dotted lines indicate the values expected from conservative mixing between fresh groundwater (triangles) and seawater (squares).

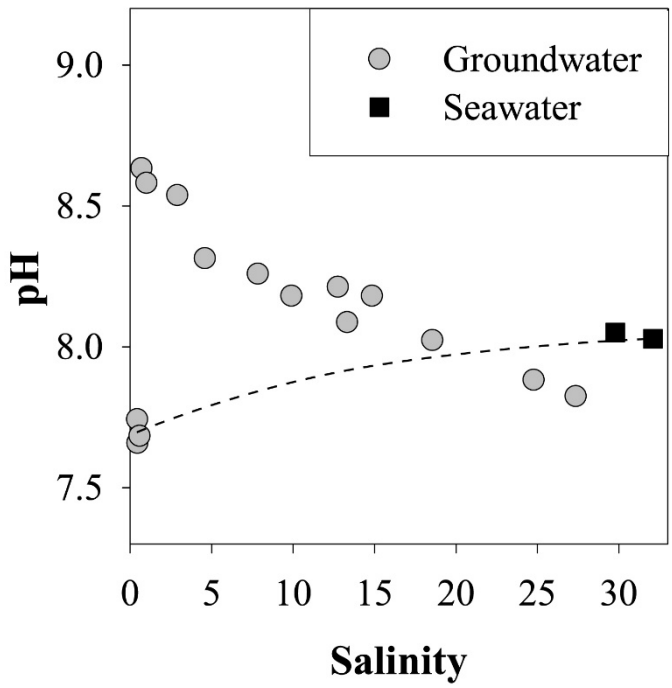

Fig. 4.5. Distributions of pH in coastal groundwater along the salinity gradients at Iho. Dotted lines indicate the values expected from conservative mixing between fresh groundwater (triangles) and seawater (squares).

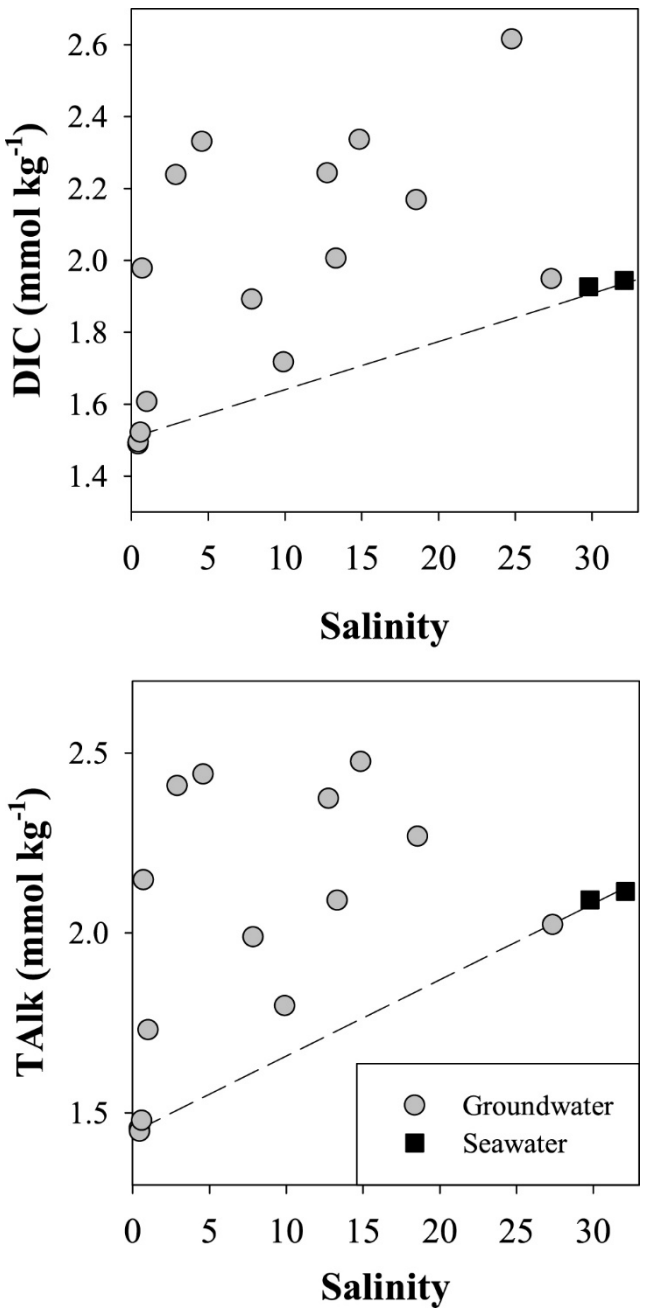

Fig. 4.6. Distributions of TAlk, and DIC in coastal groundwater along the salinity gradients at Iho. Dotted lines indicate the values expected from conservative mixing between fresh groundwater (triangles) and seawater (squares).

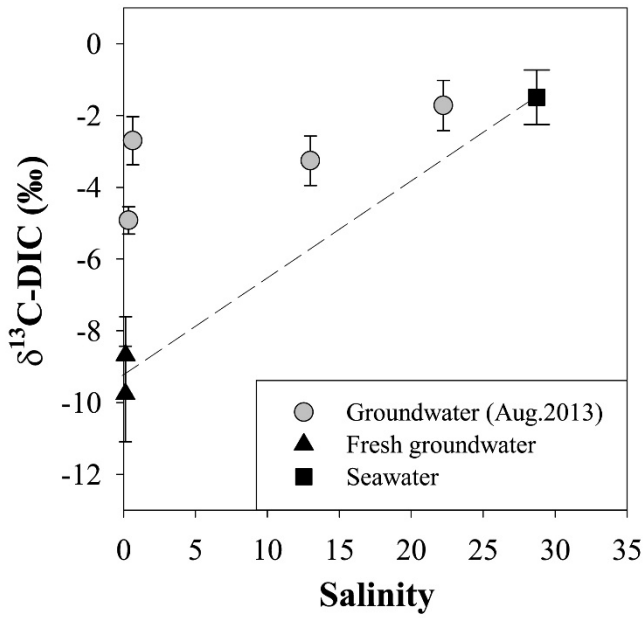

Fig. 4.7. Distributions of δ^{13}C-DIC in coastal groundwater along the salinity gradients at Hwasun Bay. Dotted lines indicate the values expected from conservative mixing between fresh groundwater (triangles) and seawater (squares).

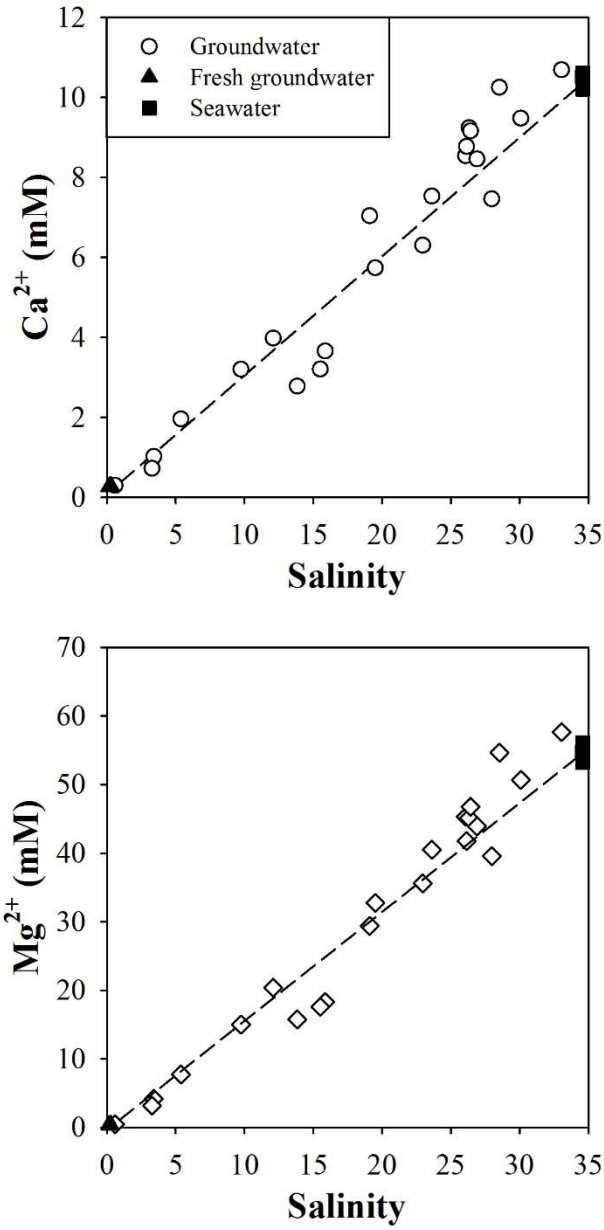

Fig. 4.8. Distributions of Ca^{2+} and Mg^{2+} in coastal groundwater along the salinity gradients at Hwasun Bay. Dotted lines indicate the values expected from conservative mixing between fresh groundwater (triangles) and seawater (squares).

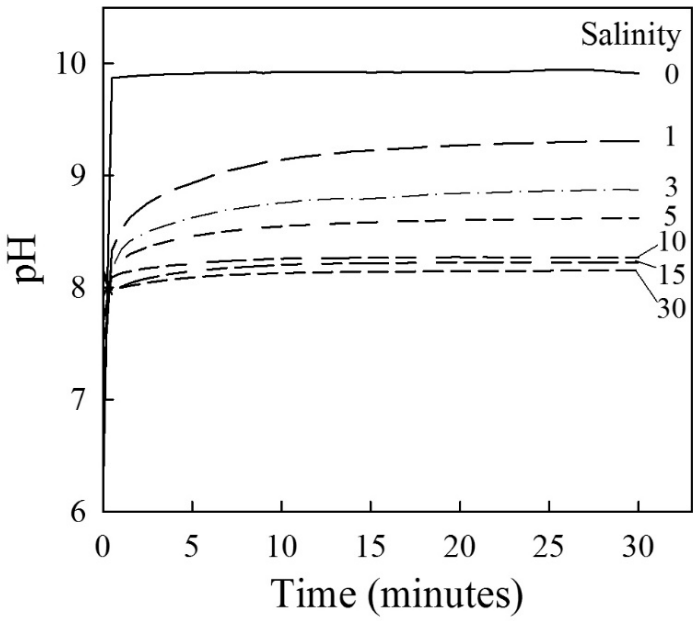

Fig. 4.9. Column experiment results: Variations in pH of different salinity waters (salinity range from 0 to 30) after passing the Hwasun sediment column.

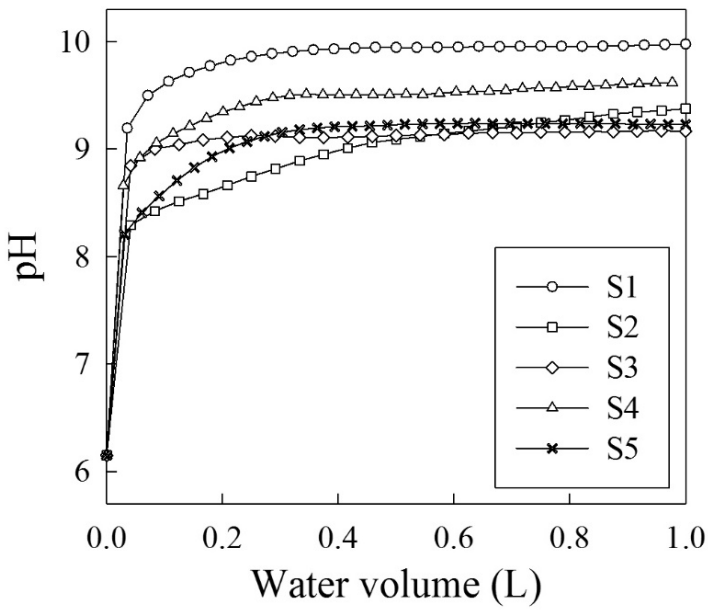

Fig. 4.10. Column experiment results: Variations in pH of deionized waters after passing the columns with different sediment samples.

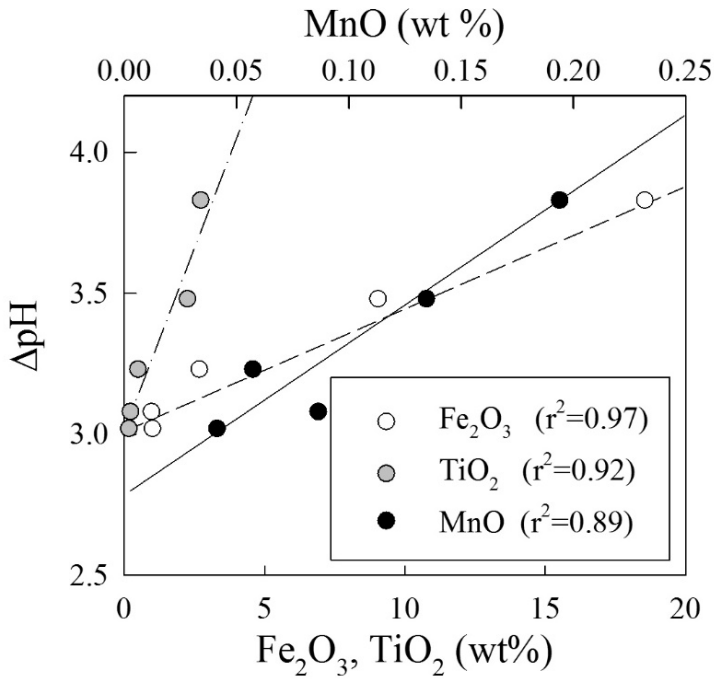

Fig. 4.11. Column experiment results: ΔpH versus the content of Fe, Ti and Mn oxides for each sediment sample.

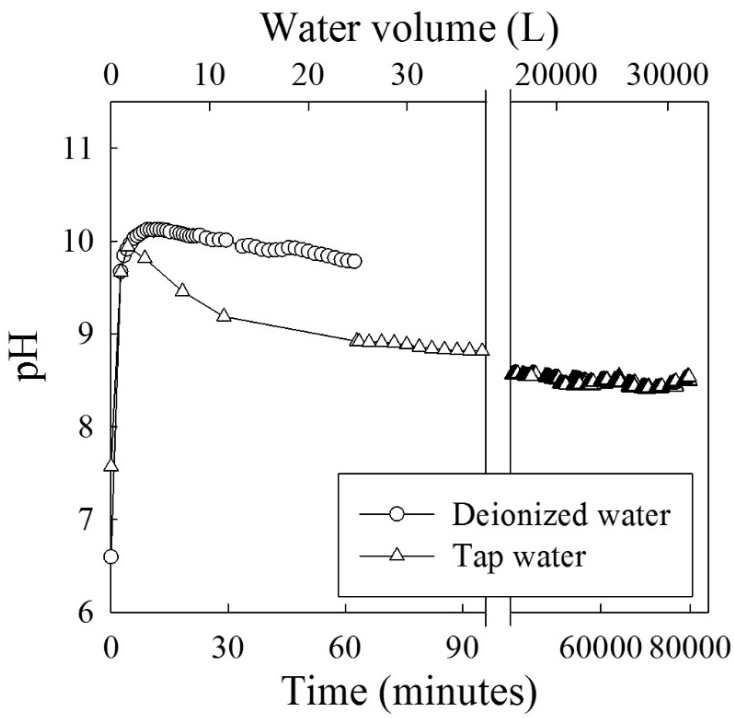

Fig. 4.12. Column experiment results: A long-term variation in pH of tap water after passing the sediment column.

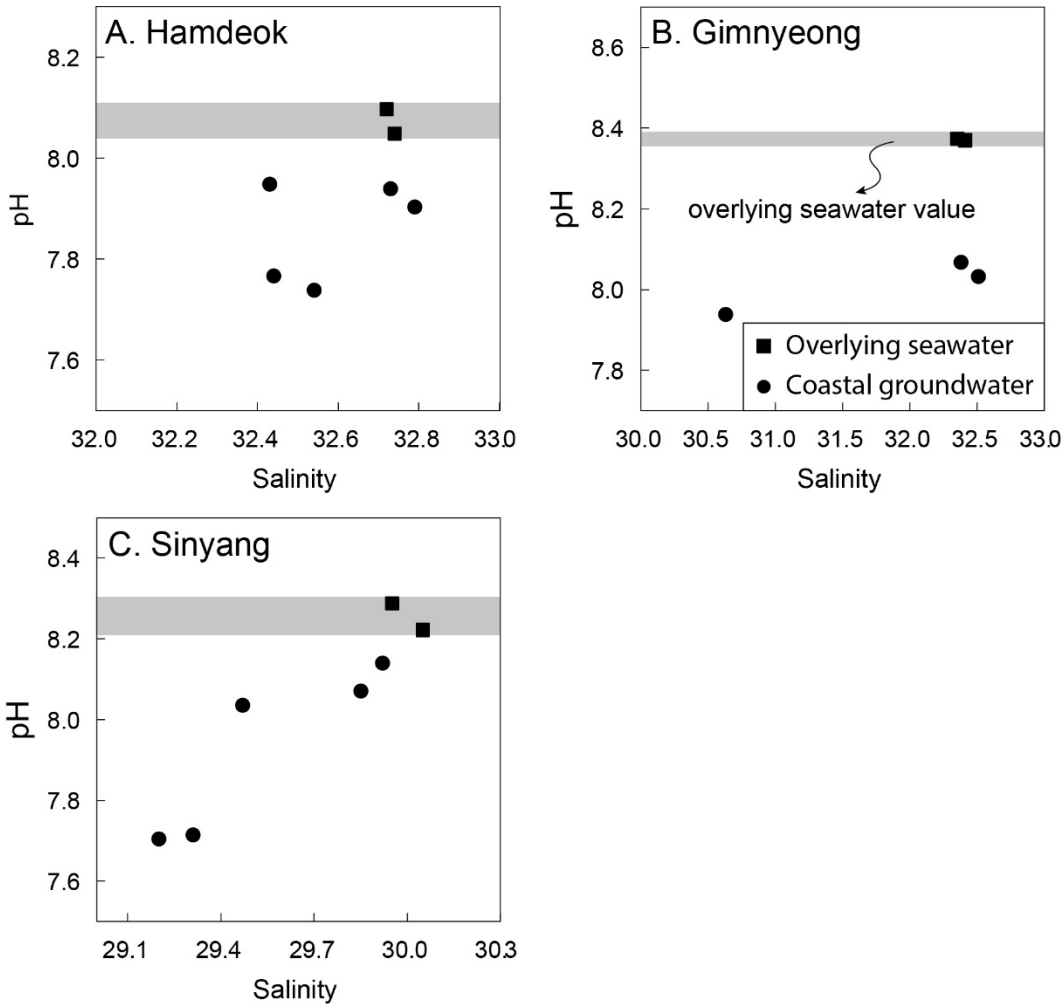

Fig. 4.13. Distributions of pH versus salinity in coastal groundwater at Hamdeok, Gimnyeong, and Sinyang. Thick gray lines indicate the pH ranges of the overlying seawater.

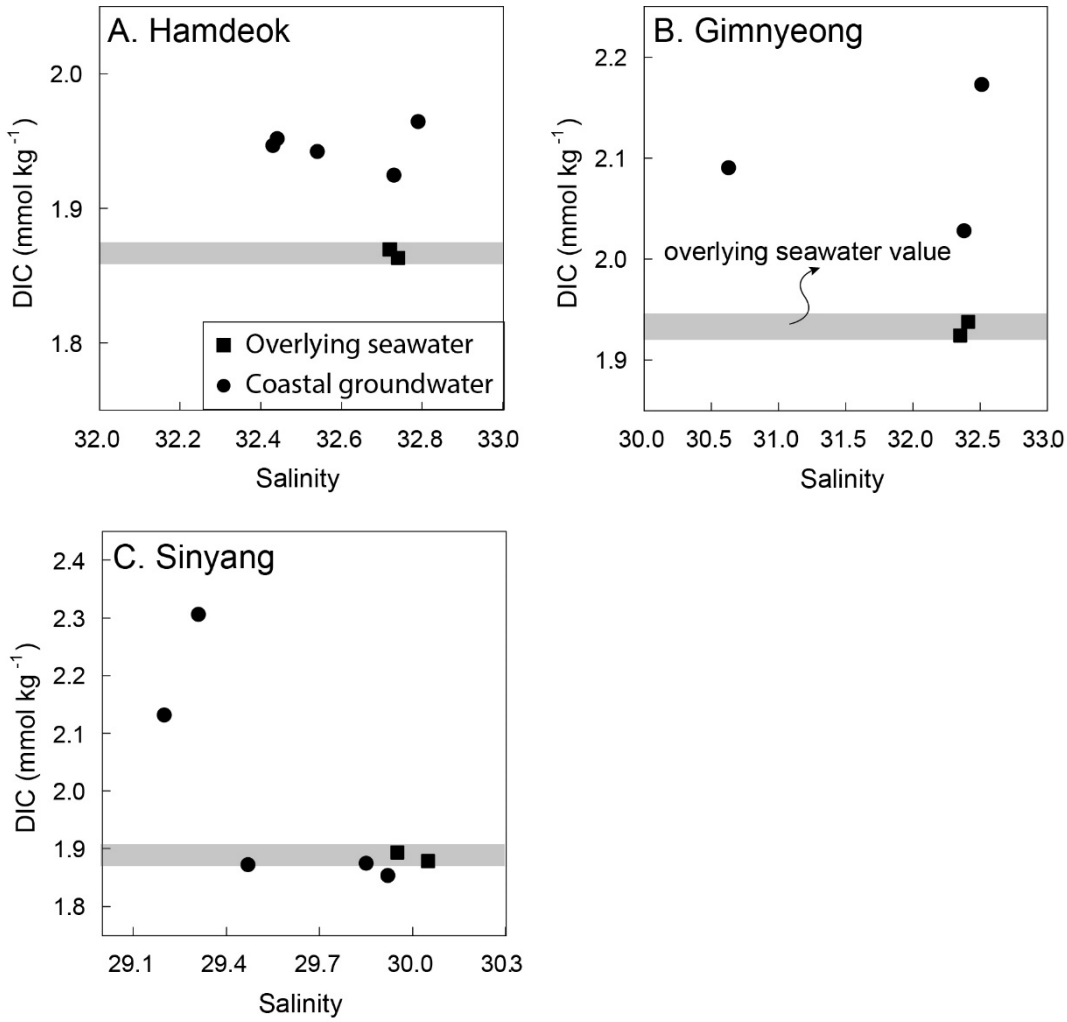

Fig. 4.14. Distributions of the DIC concentrations versus salinity in coastal groundwater at Hamdeok, Gimnyeong, and Sinyang. Thick gray lines indicate the pH ranges of the overlying seawater.

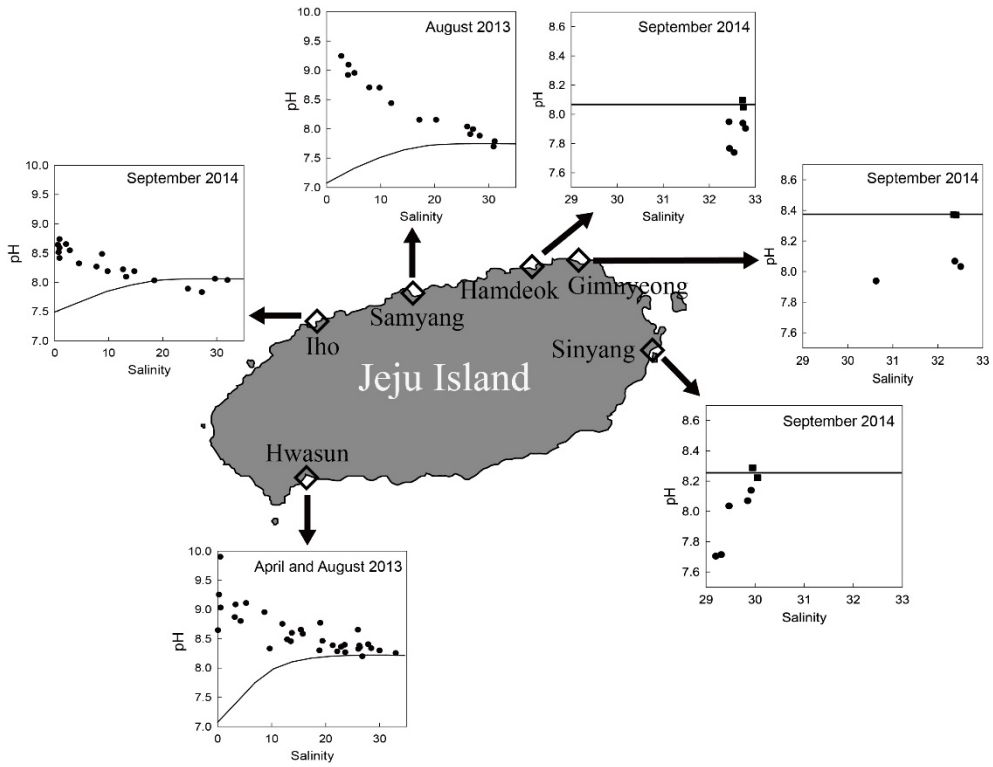

Fig. 4.15. Distributions of pH in coastal groundwater along the salinity gradients at six different sites (Hwasun, Iho, Samyang, Hamdeok, Gimnyeong, and Sinyang). Solid lines indicate the values expected from conservative mixing between fresh groundwater and seawater.

(a) Hwasun sediments

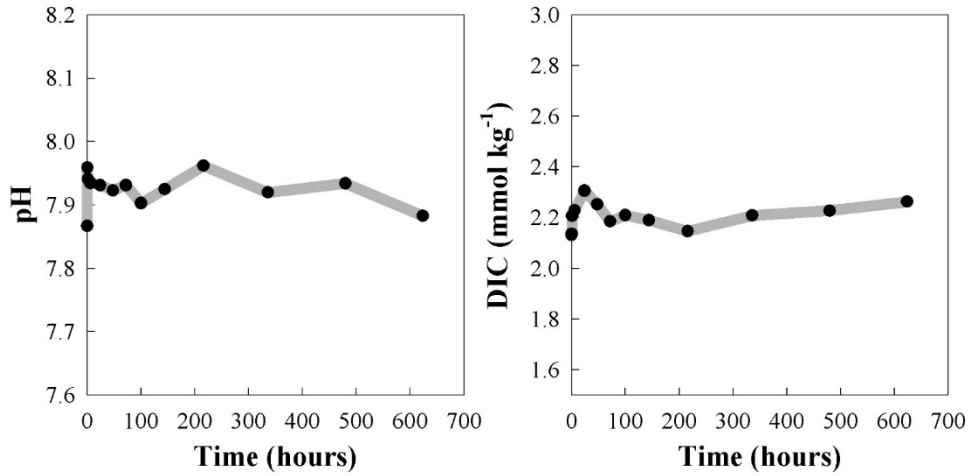

(b) Sinyang sediments

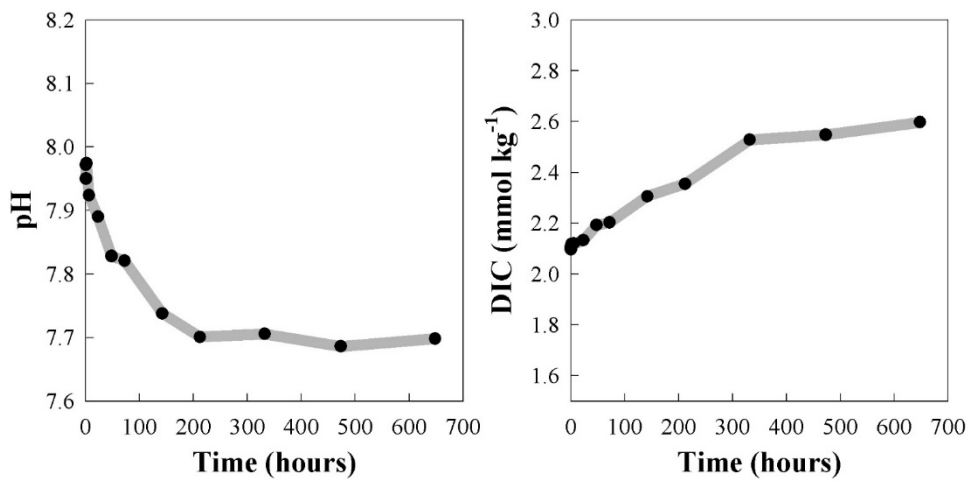

Fig. 4.16. The change in pH and DIC over time (for 30 days) of seawater incubated with sediment sample from Hwasun and Sinyang.

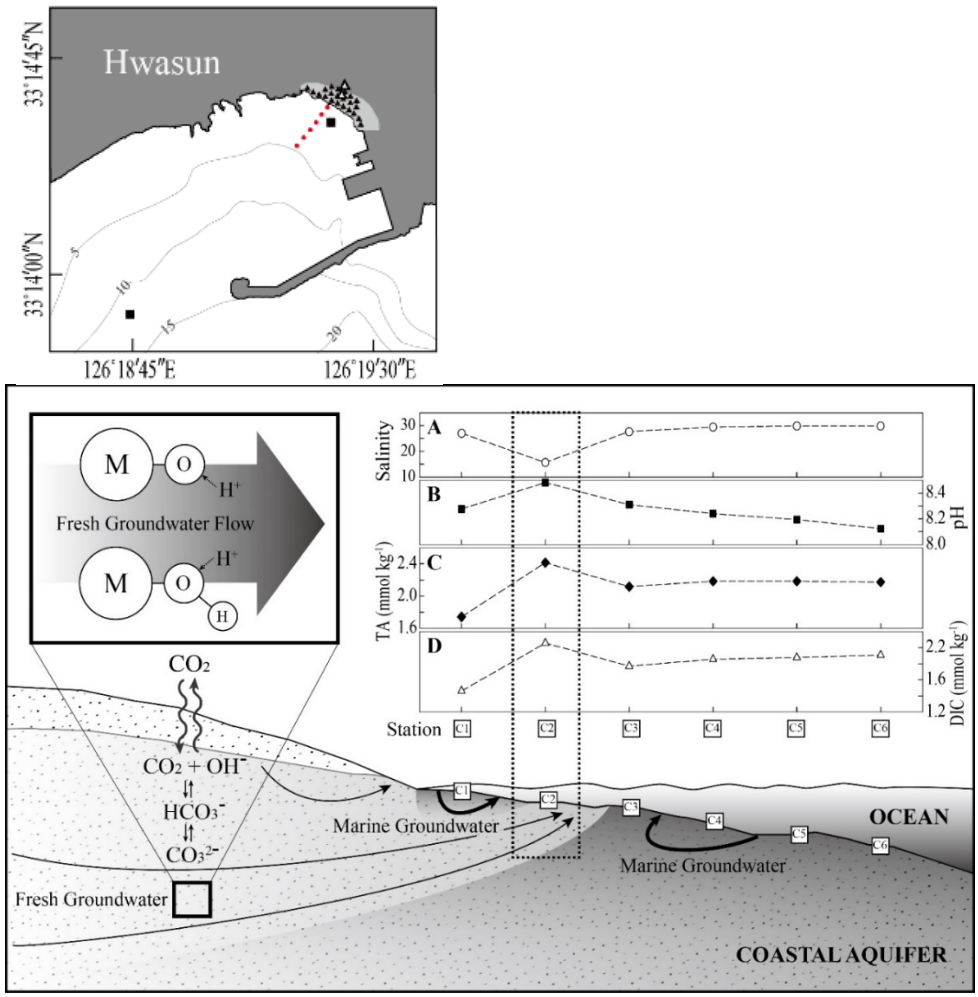

Fig. 4.17. A conceptual diagram showing the principle of the protonation of sediments and the associated carbonate systematics at Hwasun Bay, Jeju Island, Korea. The salinity, pH, TAlk, and DIC in seeping groundwater at each station (marked red dots in the map) are shown in graphs A–D, respectively.

4.2. Coastal seawater

4.2.1. pH Change Associated with Groundwater Dilution

The vertical distribution of salinity along the transect (Fig. 2.3B) showed a large lower-salinity plume (34.3–34.5), where salinities decreased toward the bottom, from 0.5 to 1.0 km off the shoreline across the entire water depth (<13 m) (Fig. 4.18A). Hwasun Bay has no surface runoff and no precipitation occurred in the three days before sampling. Therefore, these salinity anomalies mainly reflect SGD. Many submarine springs, which show lower-density water in the deeper layers, have been reported in this region as shown by Lee and Kim (2007) and Kim et al. (2011). At this plume zone, the pH (8.27–8.31) was higher than that in the other areas (8.21–8.27) (Fig. 4.18B). In contrast, the concentrations of DIC were lower than those in the other areas, and consistent with the low groundwater endmember (Fig. 4.18C). Almost no change was seen in TAlk in this lower-salinity zone. Because the pH values were calculated from DIC and TAlk concentrations, the variations in these three components are interdependent.

For the entire bay, both the pH and the DIC concentrations show significant linear correlations (r^2 = 0.82 for pH; r^2 = 0.86 for DIC) with salinity (Fig. 4.19). Because the salinity in this bay is mainly dependent on SGD, these relationships suggest that SGD dominantly affects the pH and the DIC of the seawater. The thick gray lines in Fig. 4.21 show the expected conservative mixing values for pH and DIC between the endmembers of fresh groundwater and seawater. The thicknesses of the slopes represent all possible variations of pH and DIC for the mixing between the endmembers of seawater and groundwater (Fig. 4.20). In this study, samples with

relatively higher salinities (>34.57) were assumed to be the seawater endmembers because mixing between water inside and water outside the bay is dynamic and complex. All groundwater samples for different salinities (0.3–33.1) in the STE were assumed to be the SGD endmembers because I was not aware about the actual salinities of the seeping groundwater. For groundwater, such a high pH in a low-salinity zone is likely caused by the protonation of sediments in the interface between sandy sediments and pure groundwater. In this regard, DIC and TAlk values higher than the expected values from a conservative mixing between fresh groundwater and seawater occur in the STE. The TAlk in the aquifer could be enhanced by protonation of sediments, whereas the DIC could be varied because of the subsequent CO_2 dissolution from pore air as mentioned in chapter 4.1. Simple mixing between groundwater and seawater cannot explain the positive pH anomalies (Fig. 4.21). Even if it is assumed that all of the groundwater seeping into the seawater was high pH (~10), the simple dilution by groundwater only accounts for 10% of the positive pH anomaly. Thus, such large pH increases must also result from other processes (i.e., photosynthesis and the dissolution of $CaCO_3$). The negative DIC anomalies discount a contribution from $CaCO_3$ dissolution. Therefore, the effect of photosynthesis produced by the DIN input from SGD was examined.

4.2.2. pH Change Associated with Biological Production

DIN concentrations were almost depleted (<1 μM) across most depths and sites (Fig. 4.22A), whereas DIP concentrations had slightly higher values in the low-salinity plume zone (Fig. 4.22B). The concentrations of DIN, DIP, and DSi in the coastal groundwater were 1–2 orders of magnitude higher than those in seawater

(Figs. 4.23A–C). The N:P ratios (range = 2.8–6.2; mean = 4.5 ± 1.7; n = 20) in the bay seawater were much lower than the Redfield ratio of 16 (Table 3.7). Although the change in light intensity can affect the biological production during the sampling period (8:00 a.m. – noon), the good relation between salinity and pH (with negligible DIN) indicates that the SGD-driven nutrients were fully utilized regardless of sampling time.

The expected nutrient concentrations, based on the simple-mixing model of the nutrients in SGD and seawater, are shown in Figs. 4.24. Similar to pH and DIC, the endmembers of the mixing line for groundwater represent the entire salinity range (0.3–33.1), and the seawater endmembers reflects salinity values >34.57. The results show that almost all of the SGD-driven DIN and DSi are utilized inside the bay (Figs. 4.24A and C). However, the utilization of DIP within the bay is not clear (Fig. 4.24B), perhaps because of a more significant DIP input by diffusion from the bottom sediments, as observed by Kim et al. (2011), under this extremely N-limited condition.

If it is assumed that the DIN removed from the mixing line is fully utilized by biological production, the effect of photosynthesis derived from SGD-borne nutrients on pH change can be calculated. Lee et al. (1993) and Lee et al. (1995) reported that the primary production at nearshore ranged from 0.35 to 0.61 g C m^{-2} d^{-1} in the eastern and northern coastal waters of Jeju in April 1990 and 1992 (annual variation is 0.04~1.01 g C m^{-2} d^{-1}). Thus, the increase in pH caused by biological production (estimated from DIN removal, corresponding to 0.38 g C m^{-2} d^{-1}) in the

study region is reasonable. The expected change in pH is calculated by application of the pH prediction method developed by Soetaert et al. (2007), which is adjusted on the basis of the representative concentration of DIC (2010 μmol kg^{-1}) and TAlk (2270 μmol kg^{-1}) of the offshore seawater in this region. The ΔpH and ΔDIC noted in Fig. 4.26 represent the expected change calculated by use of the Redfield ratio (C:N ratio = 6.6; Redfield [1934]) for the DIN consumption estimated in this study. This common theoretical assumption provides an explanation for the lower end of the pH and DIC anomalies (shown as the slashed area in Fig. 4.25). However, elevated C:N consumption ratios have been generally observed under N-limited conditions (Sambrotto et al., 1993; Martiny et al., 2013; Martz et al., 2014). In particular, the C:N ratios in phytoplankton are higher than 14.2 in severely N-deficient waters (Hecky et al., 1993). If it is assumed that C:N utilization ratios in this region were substantially higher (12–13) than the Redfield ratio, all of the observed values are fully explained by biological production enhanced by SGD-driven DIN.

Many factors besides SGD may influence pH in the bay seawater, including hourly variations in photosynthesis-respiration, diffusion of nutrients and CO_2 from bottom sediments, and $CaCO_3$ production-dissolution. However, these factors in this study were excluded because the factors controlling the slope of pH and DIC against salinities were examined. If they occur similarly for different salinity sites within this small sampling area, such common factors can be included in the scatter and the intercept of the plots (Fig. 4.25). Thus, it is concluded that the variations in pH and DIC across the salinity gradient were caused mainly by biological production fueled

by SGD-driven DIN.

Although these results do not cover temporal variations, the previous publications (Kim et al., 2011; Kim et al., 2013) showed similar results in this bay for SGD-driven nutrient utilization from several surveys (August 2009, October 2010, January 2011, and June 2011). All these results consistently showed that SGD-driven N flux plays a predominant role in coastal production in this oligotrophic region. Thus, the dependence of coastal water pH increases on SGD seems to be a common and perennial phenomenon in this region. However, in other regions, the effect of SGD-driven nutrient fluxes will be different, depending on oceanographic settings. For example, in the subsurface layer where re-mineralization of organic matter is more active, SGD-driven nutrients will decrease pH, similar to the subsurface layer which is greatly acidified because of riverine nutrient input (i.e., Cai et al. 2011).

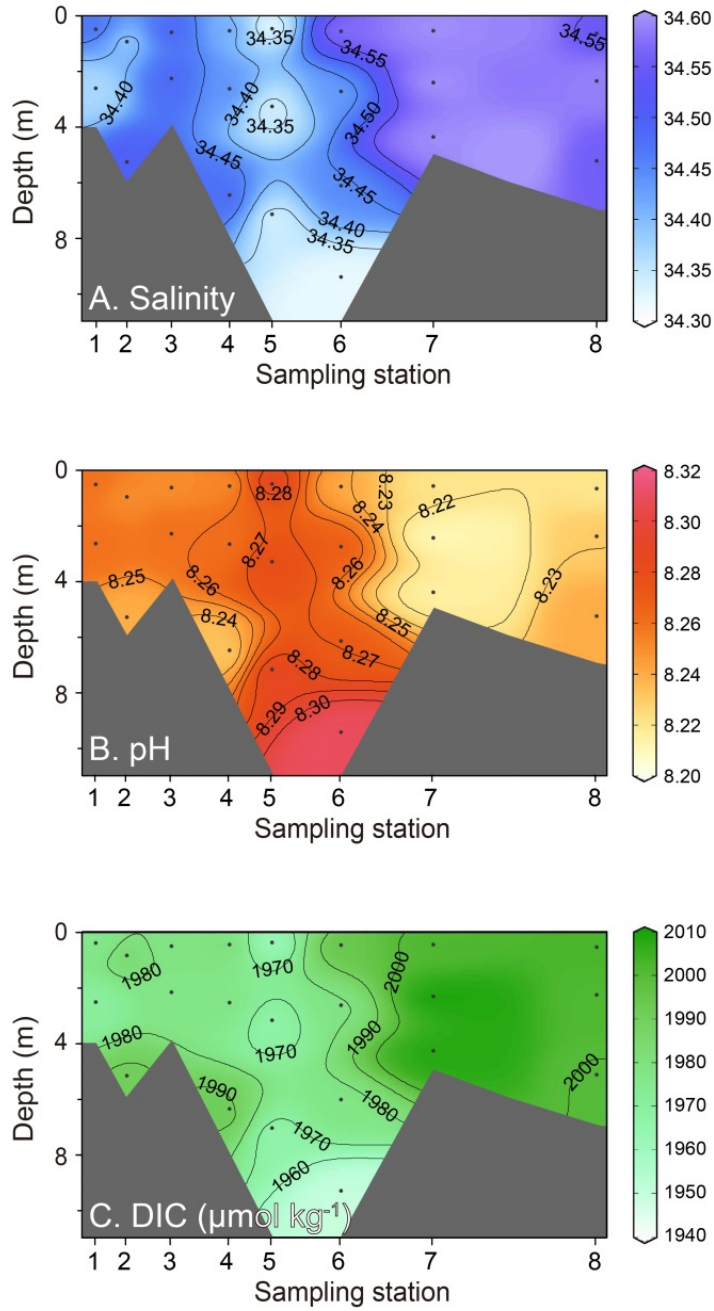

Fig. 4.18. Vertical distributions of (A) salinity, (B) pH, and (C) DIC of seawater along the transect within Hwasun Bay, Jeju Island. The transect line is shown as the gray line in Fig. 2.3.

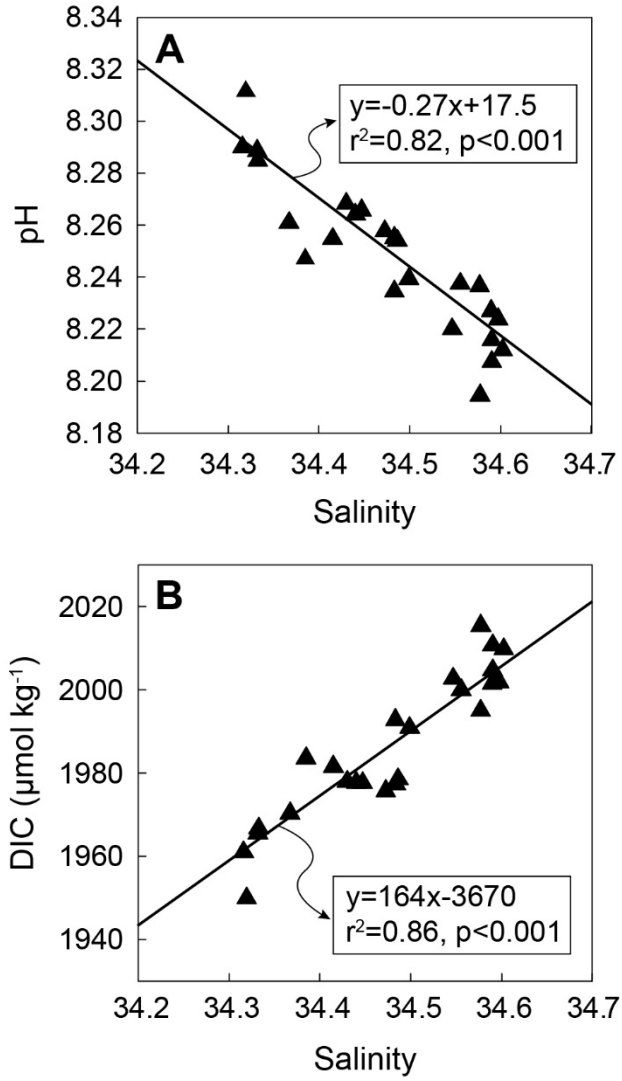

Fig. 4.19. Distributions of (A) pH and (B) DIC versus salinity of seawater in Hwasun Bay, Jeju Island.

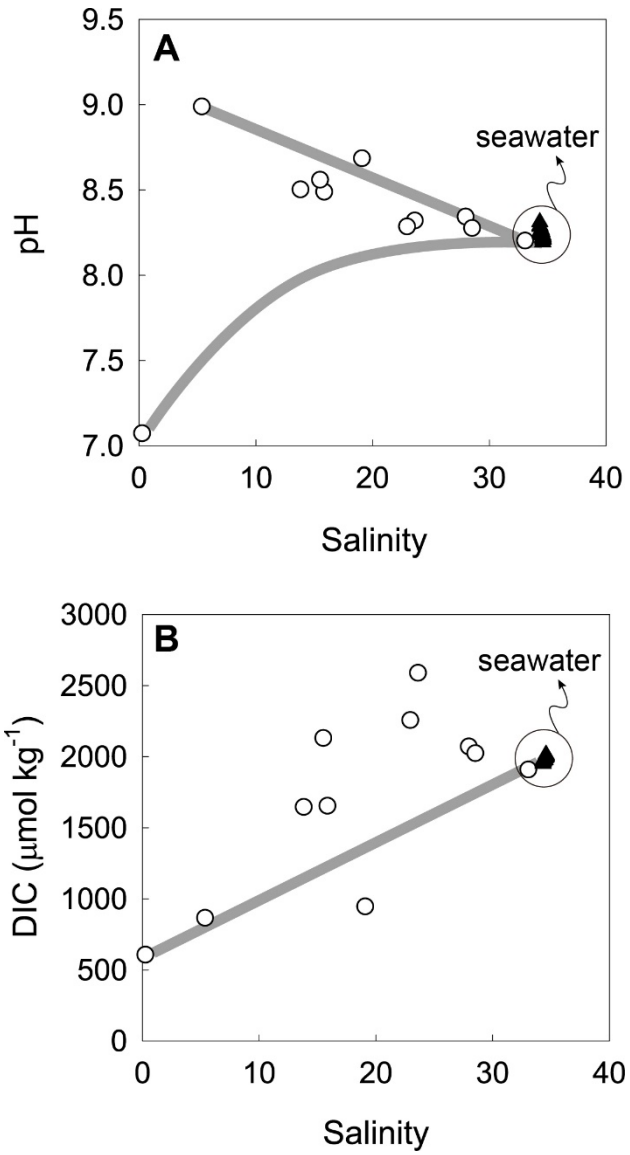

Fig. 4.20. Plots of (A) pH, and (B) DIC versus salinities of coastal groundwater sampled from the Hwasun Bay beach. Gray solid lines indicate conservative mixing between two endmembers (coastal groundwater and seawater).

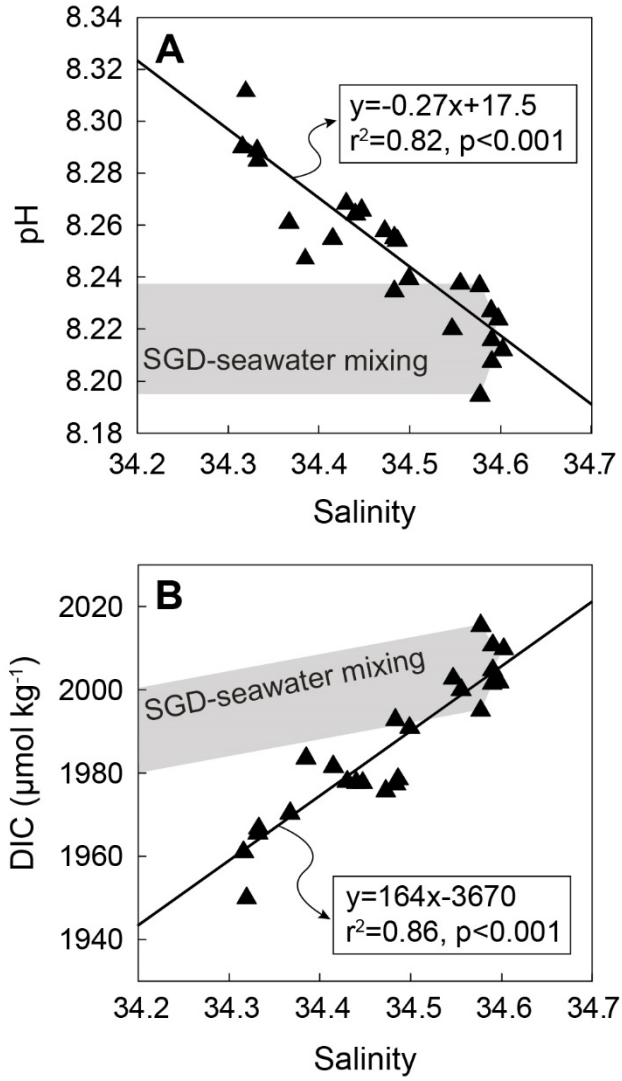

Fig. 4.21. Distributions of (A) pH and (B) DIC versus salinity of seawater in Hwasun Bay, Jeju Island. Gray solid lines (and areas) indicate the conservative mixing between two endmembers (SGD and seawater).

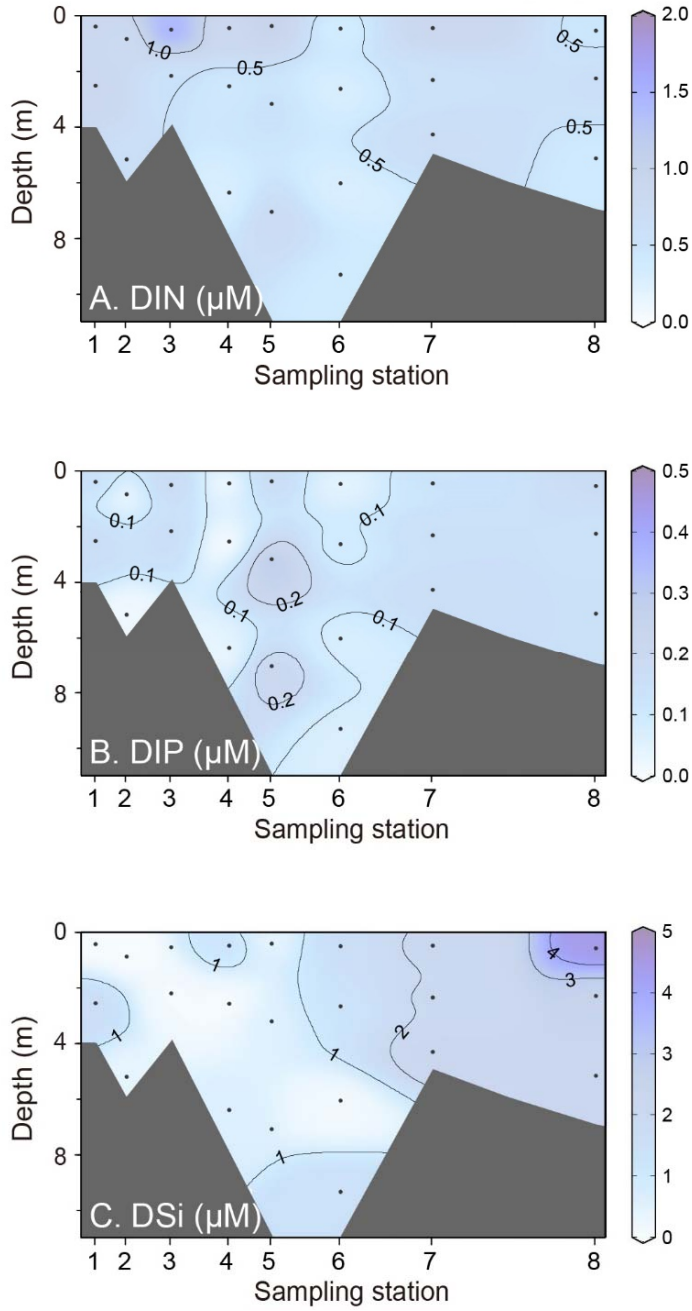

Fig. 4.22. Vertical distributions of (A) DIN, (B) DIP, and (C) DSi of seawater along the transect within Hwasun Bay, Jeju Island. The transect line is shown as the gray line in Fig.2.3.

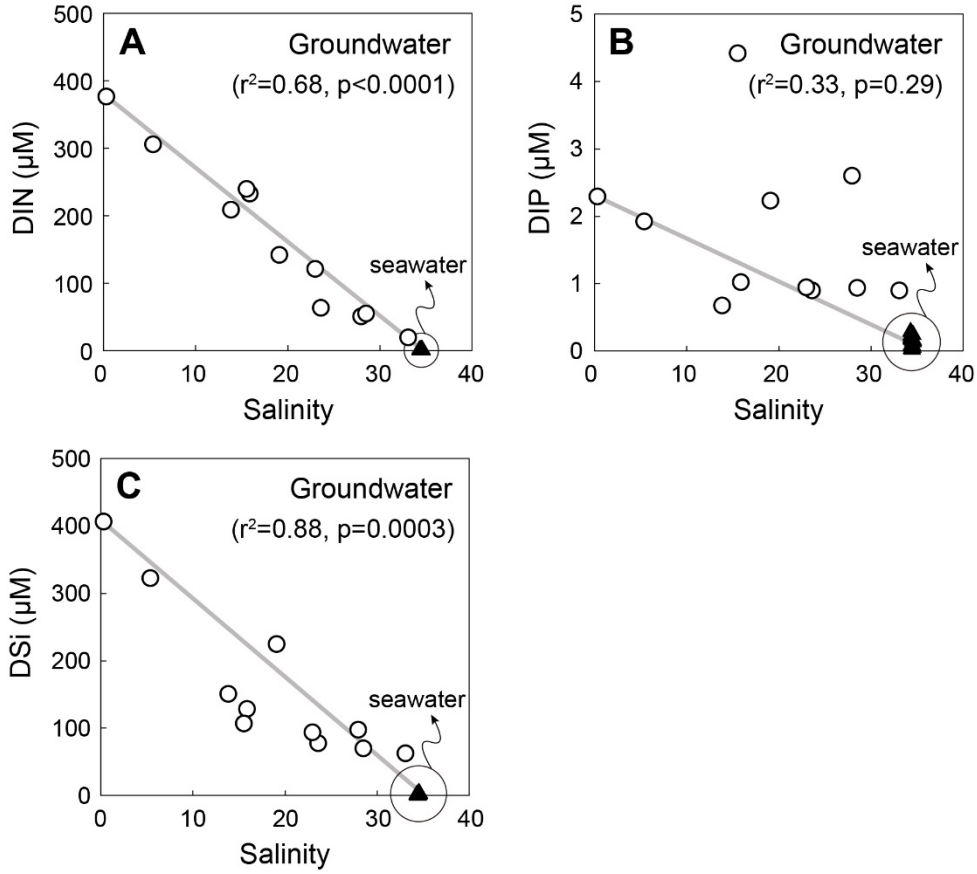

Fig. 4.23. Plots of (A) DIN, (B) DIP, and (C) DSi versus salinities of coastal groundwater sampled from the Hwasun Bay beach, Jeju Island. Gray solid lines indicate conservative mixing between two endmembers (coastal groundwater and seawater).

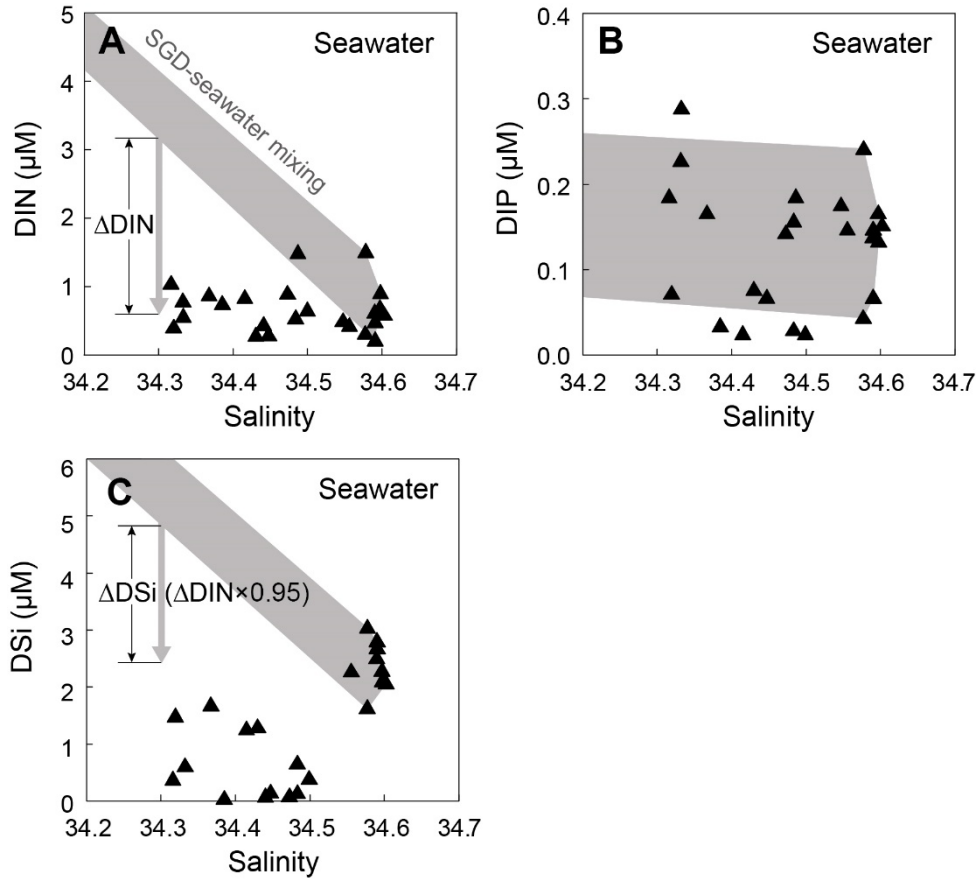

Fig. 4.24. Plots of (A) DIN, (B) DIP, and (C) DSi versus salinity of coastal seawater in Hwasun Bay, Jeju Island. Gray solid lines indicate conservative mixing between two endmembers (coastal groundwater and seawater). The ΔDIN noted in (A) indicates the amount of DIN removed from the mixing line, and the ΔDSi noted in (C) indicates the expected amount of DSi removed from the mixing line based on ΔDIN and typical nutrient stoichiometry for marine diatoms from Redfield (1934) and Brzezinski (1985).

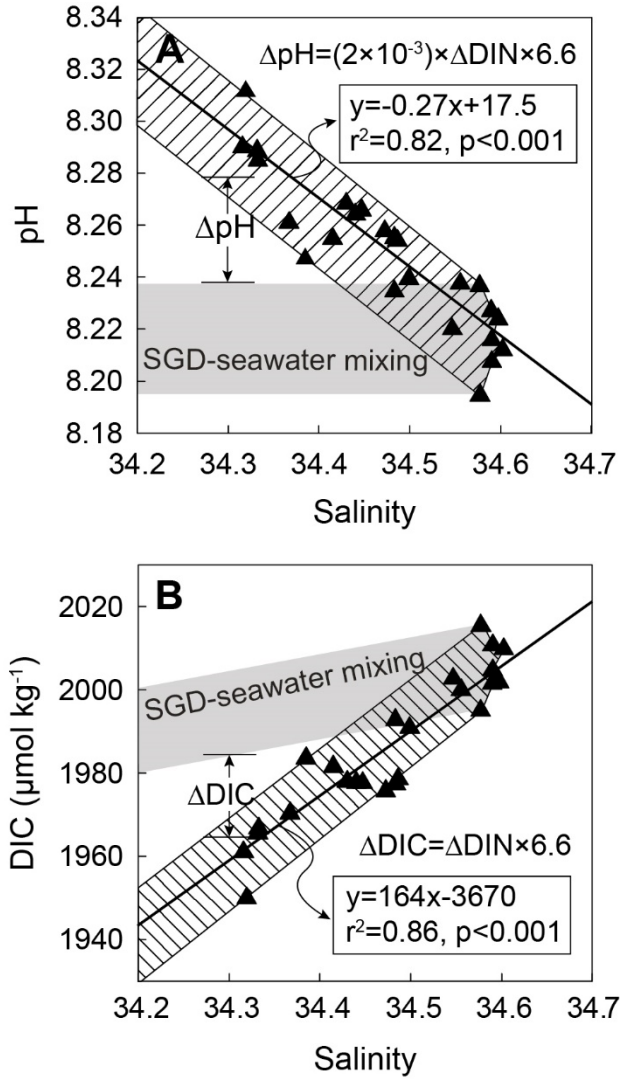

Fig. 4.25. Distributions of (A) pH and (B) DIC versus salinity of seawater in Hwasun Bay, Jeju Island. Gray solid lines (and areas) indicate the conservative mixing between two endmembers (SGD and seawater). Slashed areas indicate expected changes based on the pH prediction method (Soetaert et al., 2007), assuming that the removed DIN was fully utilized by primary production.

5. Summary and conclusion

Modern seawater acidification has been recognized to have a critical impact on ecosystems, calcite deposition, and biogeochemical cycles in the ocean (Feely et al., 2004; Orr et al., 2005; Wootton et al., 2008; Doney et al., 2009; Feely et al., 2009; Connell et al., 2013). This acidification may be further enhanced in coastal seawater and groundwater by inputs of additional acid from organic matter decomposition (Cai et al., 2003; Borges and Gypens, 2010; Cai, 2011; Cai et al., 2011). These pH changes can have critical consequences for coastal ecosystems, in addition to global ocean acidification. Rivers and coastal groundwater are major factors to control the pH in coastal ocean. While a number of studies have dealt with pH change due to nutrient inputs from rivers, studies on the effect of coastal groundwater discharge are very limited. Here, the pH change in coastal waters off an oceanic island, Jeju, where is mainly influenced by SGD on the biogeochemical cycle in coastal region, was investigated.

In this study, it is found that the protonation of sediments in coastal sandy aquifers is an important mechanism controlling pH of coastal waters, particularly off volcanic islands. These results show that protonation of sediments (adsorption of hydrogen ions onto sediments) increases pH of coastal fresh groundwater to ~10, resulting in enhanced uptake of atmospheric CO_2. However, the effect of the adsorption of protons (protonation) onto sediment minerals has never been considered as a factor controlling the pH of coastal waters. The effect of the protonation process in other areas of the global ocean is still unknown, but I believe

that this phenomenon would be more effective on volcanic islands standing in oligotrophic oceans, because of effective groundwater recharge, subsequence rapid discharge through permeable rocks, and limited accumulation of organic matter in sediments. The amount of chemical constituents (including nutrients and metals) transferred through coastal groundwater can be significantly altered by geochemical conditions, especially pH in subterranean estuaries (Slomp and Van Cappellen, 2004; Spiteri et al., 2006; Root et al., 2009). Thus, these results imply that the protonation effect on the pH of coastal waters plays an important role in coastal biogeochemical cycles, particularly on volcanic islands. In general coastal settings, the protonation effect may be exceeded by CO_2 inputs through organic matter decomposition. Thus, more intensive studies are necessary to examine the factors (i.e., salinity, organic decomposition, buffer capacity, and mineral compositions) controlling pH in subterranean waters.

In addition, a significant correlation between pH and salinity was observed in Hwasun Bay off the volcanic island, Jeju. Because the salinity anomalies within the bay are exclusively caused by SGD, the pH of the bay seawater seems to be mainly controlled by SGD and the associated biogeochemical processes. Dilution by groundwater accounts for up to 10% of the positive pH anomalies. The remaining pH change is found to be caused by enhanced biological production fueled by SGD-driven nutrients. The effect of SGD on coastal pH is clearly observed in this simple SGD-dominant system. These results suggest that the change in pH associated with SGD-driven nutrients have great impact on the acidification, deoxygenation, ecosystem changes, and biogeochemical cycles of coastal waters. Thus, extensive

studies are necessary to determine the role of SGD and SGD-driven nutrients on pH changes in coastal waters over different time and space scales.

References

Arai, Y., Sparks, D.L., Davis, J.A., 2005. Arsenate Adsorption Mechanisms at the Allophane−Water Interface. Environmental Science & Technology 39, 2537-2544.

Atkins, M.L., Santos, I.R., Ruiz-Halpern, S., Maher, D.T., 2013. Carbon dioxide dynamics driven by groundwater discharge in a coastal floodplain creek. Journal of Hydrology 493, 30-42.

Balch, W.M., Gordon, H.R., Bowler, B.C., Drapeau, D.T., Booth, E.S., 2005. Calcium carbonate measurements in the surface global ocean based on Moderate-Resolution Imaging Spectroradiometer data. Journal of Geophysical Research: Oceans 110, C07001.

Basterretxea, G., Tovar-Sanchez, A., Beck, A., Masqué, P., Bokuniewicz, H., Coffey, R., Duarte, C., Garcia-Orellana, J., Garcia-Solsona, E., Martinez-Ribes, L., Vaquer-Sunyer, R., 2010. Submarine groundwater discharge to the coastal environment of a Mediterranean Island (Majorca, Spain): Ecosystem and biogeochemical significance. Ecosystems 13, 629-643.

Borges, A.V., Frankignoulle, M., 1999. Daily and seasonal variations of the partial pressure of CO_2 in surface seawater along Belgian and southern Dutch coastal areas. Journal of Marine Systems 19, 251-266.

Borges, A.V., Gypens, N., 2010. Carbonate chemistry in the coastal zone responds more strongly to eutrophication than to ocean acidification. Limnology and Oceanography 55, 346-353.

Boutton, T.W., 1991. 11 - Stable Carbon Isotope Ratios of Natural Materials: II. Atmospheric, Terrestrial, Marine, and Freshwater Environments, in: Coleman, D.C., Fry, B. (Eds.), Carbon Isotope Techniques. Academic Press, pp. 173-185.

Brzezinski, M.A., 1985. The Si:C:N ratio of marine diatoms: Interspecific variability and the effect of some environmental variables. Journal of Phycology 21, 347-357.

Burnett, W.C., Bokuniewicz, H., Huettel, M., Moore, W.S., Taniguchi, M., 2003. Groundwater and pore water inputs to the coastal zone. Biogeochemistry 66, 3-33.

Burnett, W.C., Wattayakorn, G., Taniguchi, M., Dulaiova, H., Sojisuporn, P., Rungsupa, S., Ishitobi, T., 2007. Groundwater-derived nutrient inputs to the Upper Gulf of Thailand. Continental Shelf Research 27, 176-190.

Cai, W.-J., 2003. Riverine inorganic carbon flux and rate of biological uptake in the Mississippi River plume. Geophysical Research Letters 30, 1032.

Cai, W.-J., 2011. Estuarine and coastal ocean carbon paradox: CO_2 sinks or sites of terrestrial carbon incineration? Annual Review of Marine Science 3, 123-145.

Cai, W.-J., Hu, X., Huang, W.-J., Murrell, M.C., Lehrter, J.C., Lohrenz, S.E., Chou, W.-C., Zhai, W., Hollibaugh, J.T., Wang, Y., Zhao, P., Guo, X., Gundersen, K., Dai, M., Gong, G.-C., 2011. Acidification of subsurface coastal waters enhanced by eutrophication. Nature Geoscience 4, 766-770.

Cai, W.-J., Wang, Y., Krest, J., Moore, W.S., 2003. The geochemistry of dissolved inorganic carbon in a surficial groundwater aquifer in North Inlet, South Carolina, and the carbon fluxes to the coastal ocean. Geochimica et Cosmochimica Acta 67, 631-639.

Caldeira, K., Wickett, M.E., 2003. Oceanography: Anthropogenic carbon and ocean pH. Nature 425, 365-365.

Casey, W.H., Ludwig, C., 1996. The mechanism of dissolution of oxide minerals. Nature 381, 506-509.

Chang, K.-I., Suk, M.-S., Pang, I.-C., Teague, W., 2000. Observations of the Cheju current. JOURNAL-KOREAN SOCIETY OF OCEANOGRAPHY 35, 129-152.

Church, T.M., 1996. An underground route for the water cycle. Nature 380, 579-580.

Connell, S.D., Kroeker, K.J., Fabricius, K.E., Kline, D.I., Russell, B.D., 2013. The other ocean acidification problem: CO_2 as a resource among competitors for

ecosystem dominance. Philosophical Transactions of the Royal Society B: Biological Sciences 368, 20120442.

Cyronak, T., Santos, I.R., Erler, D.V., Eyre, B.D., 2013. Groundwater and porewater as major sources of alkalinity to a fringing coral reef lagoon (Muri Lagoon, Cook Islands). Biogeosciences 10, 2467-2480.

Davis, J.A., 1982. Adsorption of natural dissolved organic matter at the oxide/water interface. Geochimica et Cosmochimica Acta 46, 2381-2393.

Deborde, J., Anschutz, P., Auby, I., Glé, C., Commarieu, M.-V., Maurer, D., Lecroart, P., Abril, G., 2008. Role of tidal pumping on nutrient cycling in a temperate lagoon (Arcachon Bay, France). Marine Chemistry 109, 98-114.

Dickson, A.G., 1984. pH scales and proton-transfer reactions in saline media such as sea water. Geochimica et Cosmochimica Acta 48, 2299-2308.

Dickson, A.G., Millero, F.J., 1987. A comparison of the equilibrium constants for the dissociation of carbonic acid in seawater media. Deep Sea Research Part A, Oceanographic Research Papers 34, 1733-1743.

Dickson, A.G., Sabine, C.L., Christian, J.R., 2007. Guide to best practices for ocean CO_2 measurement, 3 ed. PICES Special Publication, p. 191.

Dimova, N., Dulaiova, H., Kim, G., Burnett, W.C., 2008. Uncertainties in the preparation of ^{224}Ra Mn fiber standards. Marine Chemistry 109, 220-225.

Doney, S.C., Fabry, V.J., Feely, R.A., Kleypas, J.A., 2009. Ocean Acidification: The Other CO_2 Problem. Annual Review of Marine Science 1, 169-192.

Doney, S.C., Mahowald, N., Lima, I., Feely, R.A., Mackenzie, F.T., Lamarque, J.-F., Rasch, P.J., 2007. Impact of anthropogenic atmospheric nitrogen and sulfur deposition on ocean acidification and the inorganic carbon system. Proceedings of the National Academy of Sciences 104, 14580-14585.

Dorsett, A., Cherrier, J., Martin, J.B., Cable, J.E., 2011. Assessing hydrologic and biogeochemical controls on pore-water dissolved inorganic carbon cycling in a subterranean estuary: A ^{14}C and ^{13}C mass balance approach. Marine Chemistry

127, 76-89.

Duarte, C., Hendriks, I., Moore, T., Olsen, Y., Steckbauer, A., Ramajo, L., Carstensen, J., Trotter, J., McCulloch, M., 2013. Is Ocean Acidification an Open-Ocean Syndrome? Understanding Anthropogenic Impacts on Seawater pH. Estuaries and Coasts 36, 221-236.

Feely, R.A., Alin, S.R., Newton, J., Sabine, C.L., Warner, M., Devol, A., Krembs, C., Maloy, C., 2010. The combined effects of ocean acidification, mixing, and respiration on pH and carbonate saturation in an urbanized estuary. Estuarine, Coastal and Shelf Science 88, 442-449.

Feely, R.A., Doney, S.C., Cooley, S.R., 2009. Ocean acidification: Present conditions and future changes in a high-CO_2 world. Oceanography 22, 36-47.

Feely, R.A., Sabine, C.L., Hernandez-Ayon, J.M., Ianson, D., Hales, B., 2008. Evidence for upwelling of corrosive "acidified" water onto the continental shelf. Science 320, 1490-1492.

Feely, R.A., Sabine, C.L., Lee, K., Berelson, W., Kleypas, J., Fabry, V.J., Millero, F.J., 2004. Impact of Anthropogenic CO_2 on the $CaCO_3$ System in the Oceans. Science 305, 362-366.

Frankignoulle, M., Bourge, I., Wollast, R., 1996. Atmospheric CO_2 fluxes in a highly polluted estuary (the Scheldt). Limnology and Oceanography 41, 365-369.

Frieder, C.A., Nam, S.H., Martz, T.R., Levin, L.A., 2012. High temporal and spatial variability of dissolved oxygen and pH in a nearshore California kelp forest. Biogeosciences 9, 3917-3930.

Gagan, M.K., Ayliffe, L.K., Opdyke, B.N., Hopley, D., Scott-Gagan, H., Cowley, J., 2002. Coral oxygen isotope evidence for recent groundwater fluxes to the Australian Great Barrier Reef. Geophysical Research Letters 29, 1982.

Ganor, J., Reznik, I.J., Rosenberg, Y.O., 2009. Organics in Water-Rock Interactions. Reviews in Mineralogy and Geochemistry 70, 259-369.

Gattuso, J.-P., Frankignoulle, M., Wollast, R., 1998. Carbon and carbonate

metabolism in coastal aquatic ecosystems. Annual Review of Ecology and Systematics, 405-434.

Gong, G.C., Chen, Y.L.L., Liu, K.K., 1996. Chemical hydrography and chlorophyll a distribution in the East China Sea in summer: Implications in nutrient dynamics. Continental Shelf Research 16, 1561-1590.

Guo, X., Cai, W.J., Huang, W.J., Wang, Y., Chen, F., Murrell, M.C., Lohrenz, S.E., Jiang, L.Q., Dai, M., Hartmann, J., Lin, Q., Culp, R., 2012. Carbon dynamics and community production in the Mississippi river plume. Limnology and Oceanography 57, 1-17.

Hahn, J., Lee, Y., Kim, N., Hahn, C., Lee, S., 1997. The groundwater resources and sustainable yield of Cheju volcanic island, Korea. Environmental Geology 33, 43-53.

Hecky, R.E., Cambell, P., Hendzel, L.L., 1993. The stoichiometry of carbon, nitrogen, and phosphorus in particulate matter of lakes and oceans. Limnology & Oceanography 38, 709-724.

Huang, W.J., Wang, Y., Cai, W.J., 2012. Assessment of sample storage techniques for total alkalinity and dissolved inorganic carbon in seawater. Limnology and Oceanography: Methods 10, 711-717.

Hwang, D.W., Lee, Y.W., Kim, G., 2005. Large submarine groundwater discharge and benthic eutrophication in Bangdu Bay on volcanic Jeju Island, Korea. Limnology and Oceanography 50, 1393-1403.

Jeong, H.Y., Han, Y.-S., Park, S.W., Hayes, K.F., 2010. Aerobic oxidation of mackinawite (FeS) and its environmental implication for arsenic mobilization. Geochimica et Cosmochimica Acta 74, 3182-3198.

Jeong, J., Kim, G., Han, S., 2012. Influence of trace element fluxes from submarine groundwater discharge (SGD) on their inventories in coastal waters off volcanic island, Jeju, Korea. Applied Geochemistry 27, 37-43.

Johnson, A.G., Glenn, C.R., Burnett, W.C., Peterson, R.N., Lucey, P.G., 2008. Aerial

infrared imaging reveals large nutrient-rich groundwater inputs to the ocean. Geophysical Research Letters 35, L15606.

Kim, G., Kim, J.S., Hwang, D.W., 2011. Submarine groundwater discharge from oceanic islands standing in oligotrophic oceans: Implications for global biological production and organic carbon fluxes. Limnology and Oceanography 56, 673-682.

Kim, G., Lee, K.-K., Park, K.-S., Hwang, D.-W., Yang, H.-S., 2003. Large submarine groundwater discharge (SGD) from a volcanic island. Geophysical Research Letters 30, 2098.

Kim, G., Ryu, J.-W., Hwang, D.-W., 2008a. Radium tracing of submarine groundwater discharge (SGD) and associated nutrient fluxes in a highly-permeable bed coastal zone, Korea. Marine Chemistry 109, 307-317.

Kim, G., Swarzenski, P.W., 2010. Submarine Groundwater Discharge (SGD) and Associated Nutrient Fluxes to the Coastal Ocean, in: Liu, K.-K., Atkinson, L., Quiñones, R., Talaue-McManus, L. (Eds.), Carbon and Nutrient Fluxes in Continental Margins. Springer Berlin Heidelberg, pp. 529-538.

Kim, I., Kim, G., 2011. Large fluxes of rare earth elements through submarine groundwater discharge (SGD) from a volcanic island, Jeju, Korea. Marine Chemistry 127, 12-19.

Kim, T.-H., Kwon, E., Kim, I., Lee, S.-A., Kim, G., 2013. Dissolved organic matter in the subterranean estuary of a volcanic island, Jeju: Importance of dissolved organic nitrogen fluxes to the ocean. Journal of Sea Research 78, 18-24.

Kim, T.H., Nam, J.M., Ge, L., Lee, K.I., 2008b. Settlement Characteristic of Beach Sands and Its Evaluation. Marine Georesources & Geotechnology 26, 67-85.

Kleypas, J.A., Feely, R.A., Fabry, V.J., Langdon, C., Sabine, C.L., Robbins, L.L., 2005. Impacts of ocean acidification on coral reefs and other marine calcifiers: a guide for future research, Report of a workshop held. Citeseer, p. e20.

Koh, D.-C., Plummer, L.N., Busenberg, E., Kim, Y., 2007. Evidence for terrigenic

SF_6 in groundwater from basaltic aquifers, Jeju Island, Korea: Implications for groundwater dating. Journal of Hydrology 339, 93-104.

Kung, H.H., 1989. Transition metal oxides: surface chemistry and catalysis. Elsevier.

Kwon, E.Y., Kim, G., Primeau, F., Moore, W.S., Cho, H.-M., DeVries, T., Sarmiento, J.L., Charette, M.A., Cho, Y.-K., 2014. Global estimate of submarine groundwater discharge based on an observationally constrained radium isotope model. Geophysical Research Letters, 2014GL061574.

Lee, J.-M., Kim, G., 2007. Estimating submarine discharge of fresh groundwater from a volcanic island using a freshwater budget of the coastal water column. Geophysical Research Letters 34, L11611.

Lee, J., Choa, J., Go, Y., Choi, Y., 1993. Bioecological studies of the eastern coastal area in Cheju Island (II). Phytoplankton dynamics and primary productivity around U-do. J. Korean Earth Sci. Soc 14, 458-466.

Lee, J.B., Koh, H.B., Go, Y.B., Choi, Y.C., 1995. Bioecological studies of the northern coastal area in Cheju Island: Phytoplankton dynamics and primary productivity at the Hamdeok area. Bulletin of Marine Research, Institute of Cheju National University 19, 103-113.

Lee, Y.-W., Lee, J.-M., Kim, G., 2009. Identifying sharp hydrographical changes in phytoplankton community structure using HPLC pigment signatures in coastal waters along Jeju Island, Korea. Ocean Science Journal 44, 1-10.

Lewis, E., Wallace, D.W.R., 1998. Program developed for CO_2 system calculations. Oak Ridge National Laboratory, Oak Ridge.

Liu, Q., Dai, M., Chen, W., Huh, C.A., Wang, G., Li, Q., Charette, M.A., 2012. How significant is submarine groundwater discharge and its associated dissolved inorganic carbon in a river-dominated shelf system? Biogeosciences 9, 1777-1795.

Maher, D.T., Santos, I.R., Golsby-Smith, L., Gleeson, J., Eyre, B.D., 2013. Groundwater-derived dissolved inorganic and organic carbon exports from a

mangrove tidal creek: The missing mangrove carbon sink? Limnology and Oceanography 58, 475-488.

Martiny, A.C., Pham, C.T.A., Primeau, F.W., Vrugt, J.A., Moore, J.K., Levin, S.A., Lomas, M.W., 2013. Strong latitudinal patterns in the elemental ratios of marine plankton and organic matter. Nature Geosci 6, 279-283.

Martz, T., Send, U., Ohman, M.D., Takeshita, Y., Bresnahan, P., Kim, H.-J., Nam, S., 2014. Dynamic variability of biogeochemical ratios in the Southern California Current System. Geophysical Research Letters 41, 2014GL059332.

Mehrbach, C., Culberson, C.H., Hawley, J.E., Pytkowicz, R.M., 1973. Measurement of the apparent dissociation constants of carbonic acid in seawater at atmospheric pressure. Limnology and Oceanography 18, 897-907.

Melzner, F., Thomsen, J., Koeve, W., Oschlies, A., Gutowska, M.A., Bange, H.W., Hansen, H.P., Körtzinger, A., 2013. Future ocean acidification will be amplified by hypoxia in coastal habitats. Marine Biology 160, 1875-1888.

Millero, F.J., 1995. Thermodynamics of the carbon dioxide system in the oceans. Geochimica et Cosmochimica Acta 59, 661-677.

Moore, W.S., Blanton, J.O., Joye, S.B., 2006. Estimates of flushing times, submarine groundwater discharge, and nutrient fluxes to Okatee Estuary, South Carolina. Journal of Geophysical Research: Oceans 111, C09006.

Ning, X., Liu, Z., Cai, Y., Fang, M., Chai, F., 1998. Physicobiological oceanographic remote sensing of the East China Sea: Satellite and in situ observations. Journal of Geophysical Research: Oceans 103, 21623-21635.

Orr, J.C., Fabry, V.J., Aumont, O., Bopp, L., Doney, S.C., Feely, R.A., Gnanadesikan, A., Gruber, N., Ishida, A., Joos, F., Key, R.M., Lindsay, K., Maier-Reimer, E., Matear, R., Monfray, P., Mouchet, A., Najjar, R.G., Plattner, G.-K., Rodgers, K.B., Sabine, C.L., Sarmiento, J.L., Schlitzer, R., Slater, R.D., Totterdell, I.J., Weirig, M.-F., Yamanaka, Y., Yool, A., 2005. Anthropogenic ocean acidification over the twenty-first century and its impact on calcifying organisms. Nature 437, 681-686.

Paytan, A., Shellenbarger, G.G., Street, J.H., Gonneea, M.E., Davis, K., Young, M.B., Moore, W.S., 2006. Submarine groundwater discharge: An important source of new inorganic nitrogen to coral reef ecosystems. Limnology and Oceanography 51, 343-348.

Provoost, P., van Heuven, S., Soetaert, K., Laane, R.W.P.M., Middelburg, J.J., 2010. Seasonal and long-term changes in pH in the Dutch coastal zone. Biogeosciences 7, 3869-3878.

Redfield, A.C., 1934. On the proportions of organic derivatives in sea water and their relation to the composition of plankton, in: Daniel, R.J. (Ed.), James Johnstone Memorial Volume. University Press of Liverpool, pp. 177-192.

Root, R.A., Vlassopoulos, D., Rivera, N.A., Rafferty, M.T., Andrews, C., O'Day, P.A., 2009. Speciation and natural attenuation of arsenic and iron in a tidally influenced shallow aquifer. Geochimica et Cosmochimica Acta 73, 5528-5553.

Sabine, C.L., Feely, R.A., Gruber, N., Key, R.M., Lee, K., Bullister, J.L., Wanninkhof, R., Wong, C.S., Wallace, D.W.R., Tilbrook, B., Millero, F.J., Peng, T.-H., Kozyr, A., Ono, T., Rios, A.F., 2004. The Oceanic Sink for Anthropogenic CO_2. Science 305, 367-371.

Salisbury, J., Green, M., Hunt, C., Campbell, J., 2008. Coastal Acidification by Rivers:A Threat to Shellfish? Eos, Transactions American Geophysical Union 89, 513-513.

Sambrotto, R.N., Savidge, G., Robinson, C., Boyd, P., Takahashi, T., Karl, D.M., Langdon, C., Chipman, D., Marra, J., Codispoti, L., 1993. Elevated consumption of carbon relative to nitrogen in the surface ocean. Nature 363, 248-250.

Santos, I.R., Burnett, W.C., Chanton, J., Mwashote, B., Suryaputra, I.G.N.A., Dittmar, T., 2008. Nutrient biogeochemistry in a Gulf of Mexico subterranean estuary and groundwater-derived fluxes to the coastal ocean. Limnology and Oceanography 53, 705-718.

Schott, J., Pokrovsky, O.S., Oelkers, E.H., 2009. The Link Between Mineral

Dissolution/Precipitation Kinetics and Solution Chemistry. Reviews in Mineralogy and Geochemistry 70, 207-258.

Singurindy, O., Berkowitz, B., Lowell, R.P., 2004. Carbonate dissolution and precipitation in coastal environments: Laboratory analysis and theoretical consideration. Water Resources Research 40, n/a-n/a.

Slomp, C.P., Van Cappellen, P., 2004. Nutrient inputs to the coastal ocean through submarine groundwater discharge: controls and potential impact. Journal of Hydrology 295, 64-86.

Smedley, P.L., Kinniburgh, D.G., 2002. A review of the source, behaviour and distribution of arsenic in natural waters. Applied Geochemistry 17, 517-568.

Soetaert, K., Hofmann, A.F., Middelburg, J.J., Meysman, F.J.R., Greenwood, J., 2007. The effect of biogeochemical processes on pH. Marine Chemistry 105, 30-51.

Spiteri, C., Regnier, P., Slomp, C.P., Charette, M.A., 2006. pH-Dependent iron oxide precipitation in a subterranean estuary. Journal of Geochemical Exploration 88, 399-403.

St-Jean, G., 2003. Automated quantitative and isotopic (^{13}C) analysis of dissolved inorganic carbon and dissolved organic carbon in continuous-flow using a total organic carbon analyser. Rapid communications in mass spectrometry 17, 419-428.

Stumm, W., Morgan, J.J., 1996. Aquatic chemistry: chemical equilibria and rates in natural waters, 3rd ed. John Wiley & Sons, Inc.

Szymczycha, B., Maciejewska, A., Szczepanska, A., Pempkowiak, J., 2013. The submarine groundwater discharge as a carbon source to the Baltic Sea. Biogeosciences Discussions 10, 2069-2091.

Waldbusser, G.G., Voigt, E.P., Bergschneider, H., Green, M.A., Newell, R.I.E., 2011. Biocalcification in the Eastern Oyster (Crassostrea virginica) in Relation to Long-term Trends in Chesapeake Bay pH. Estuaries and Coasts 34, 221-231.

Waska, H., Kim, G., 2011. Submarine groundwater discharge (SGD) as a main nutrient source for benthic and water-column primary production in a large intertidal environment of the Yellow Sea. Journal of Sea Research 65, 103-113.

Waters, J.F., Millero, F.J., 2013. The free proton concentration scale for seawater pH. Marine Chemistry 149, 8-22.

Won, J.H., Kim, J.W., Koh, G.W., Lee, J.Y., 2005. Evaluation of hydrogeological characteristics in Jeju Island, Korea. Geosciences Journal 9, 33-46.

Won, J.H., Lee, J.Y., Kim, J.W., Koh, G.W., 2006. Groundwater occurrence on Jeju Island, Korea. Hydrogeology Journal 14, 532-547.

Wootton, J.T., Pfister, C.A., 2012. Carbon System Measurements and Potential Climatic Drivers at a Site of Rapidly Declining Ocean pH. PLoS ONE 7, 11.

Wootton, J.T., Pfister, C.A., Forester, J.D., 2008. Dynamic patterns and ecological impacts of declining ocean pH in a high-resolution multi-year dataset. Proceedings of the National Academy of Sciences of the United States of America 105, 18848-18853.

Zhang, J., Quay, P.D., Wilbur, D.O., 1995. Carbon isotope fractionation during gas-water exchange and dissolution of CO_2. Geochimica et Cosmochimica Acta 59, 107-114.

국문초록

인간의 산업활동으로 인한 대기 중 이산화탄소의 증가는 전 지구적으로 해양 산성화를 초래하고 있다. 대양 표층의 pH는 산업혁명 이전보다 약 0.1 감소하였으며, 일부 연안 해수의 경우에는 그 감소 추세가 더욱 심각하다. 이러한 해양 산성화는 해양 생태계 및 생지화학적 순환에 심각한 결과를 초래한다. 강물에 의한 영양염의 과유입은 표층 해수의 pH를 높이고, 이로부터 증가한 유기 물질의 분해로 인하여 연안의 저층 해수는 대양보다 더 빠른 속도로 산성화가 일어나기도 한다. 강물을 통한 영양염 유입에 의한 연안 해수의 산성화에 관한 연구는 과거부터 매우 많이 이루어지고 있지만, 최근 연안의 주요한 영양염 공급원으로 알려진 해저 지하수에 의한 연안 산성화에 관한 연구는 매우 부족하다.

따라서 본 연구에서는, 해저 담 지하수 및 염 지하수의 영향이 뚜렷한 화산섬에서 연안 지하수의 pH에 관하여 고찰하였다. 제주도 남서쪽에 위치한 화순만의 해저 하구로부터 지하수를 채취하여 pH (NBS 스케일), 총 무기탄소(dissolved inorganic carbon: DIC), 총 알칼리도 (total alkalinity: TAlk), 탄소동위원소(δ^{13}C-DIC), 및 칼슘과 마그네슘 이온의 농도를 측정하였다. 모래 퇴적층으로 이루어진 화순만의 해저 하구를 흐르는 지하수의 pH는 육상 담 지하수가 해저 하구로 유입되자 그 pH 값은 7.4(±0.2)으로부터 10까지 급격하게 증가된 후, 유입된 해수와 보존적으로 혼합되는 양상을 보였다. 제주 북부의 삼양과 제주 북서부의 이호에서도 이와 유사한 패턴을 보였다. 화순에서 채취한 해저 지하수 시료의 δ^{13}C-DIC, 칼슘 이온(Ca^{2+}) 및 마그네슘 이온(Mg^{2+}) 측정 결과와 모래 퇴적물 실험 결과로부터, 담 지하수의 급격한 pH의 증가는 제주

지역 퇴적물의 양성자 흡착 반응(adsorption of protons onto sandy sediments; protonation of sediments)에 의한 것임을 밝혀내었다. 제주도의 다섯 지역(화순, 삼양, 협재, 함덕, 표선)으로부터 채취한 각기 다른 퇴적물을 이용한 다양한 실험실 실험 결과, 퇴적물의 양성자 흡착 반응은 (1) 제주의 다양한 지역의 퇴적물에서 공통적으로 일어나며, (2) 염분 10 이하의 담 지하수에서만 pH의 증가가 뚜렷이 보이며, (3) 퇴적물의 전이금속 (예, Fe, Ti 및 Mn) 산화물의 함량이 높을수록 효과적으로 일어남을 알 수 있었다. 해수와 지하수가 혼합되어 서서히 유출되는 지하수(seeping groundwater)를 채취하여 측정한 결과, 모래 퇴적층에서 증가된 pH가 높은 알칼리성의 지하수가 연안 해수로 직접 유입되고 있음을 알 수 있었다. 양성자 흡착 반응으로 인한 연안 지하수의 pH 증가는 대기 중 CO_2를 효과적으로 흡수하는 요인으로 작용하기도 한다. 본 연구에서는 제주 지역의 연안 지하수와 퇴적층의 상호 작용이 해저 하구의 pH를 급격히 변화시키는 현상을 밝혀내었고, 이는 pH에 민감하게 반응하는 해저 하구 내의 물질 거동을 이해하는데 주요한 밑거름이 될 것이다. 양성자 흡착 반응에 의한 pH 변화는 제주 전 지역에서 보인다. 그러나 유기물 함량이 퇴적층을 가지는 일부 지역의 경우에는 해저 지하수가 해저 하구 퇴적층에서 느리게 흐를수록 유기물 분해에 의하여 약 7.7까지 pH가 감소함과 동시에 약 2.5 mmol kg^{-1}까지 용존 무기탄소가 증가하는 양상을 보인다. 제주 지역 연안 지하수의 pH 변화는 양성자 흡착 반응에 의한 pH 증가와 유기물 분해에 의한 pH 감소의 두 요인에 의한 것으로 보인다.

이와 함께, 본 연구에서는 연안 지하수의 유출이 빈 영양 유역인 화산섬 연안 해수의 pH에 어떠한 영향을 미치는지에 관하여 고찰하였다. 화순만 해수의 염분은 하천의 유입이 없어 전적으로 해저 지하수의

유입에 의존하는데, 수평 약 0.5 km 규모로 바닥에서 표층으로 상승하는 저염 수괴(low-salinity plume)가 존재함을 발견하였다. 이 때, 화순만 해수 전체의 염분에 따른 pH를 도시해보면, 염분과 pH는 뚜렷한 음의 상관관계(r^2=0.82)를 보인다. 해저 지하수와 외해의 두 단성분(end-member)의 혼합 모델을 적용하면, 이러한 음의 상관관계는 해저 지하수와 해수의 단순 혼합에 의한 결과가 아니라 해저 지하수로부터 공급된 영양염에 의한 생물 생산의 결과임을 알 수 있었다. 연안 지역의 해저 지하수에 의한 영양염 공급량이 강물에 의한 공급량과 유사하거나 이보다 더 높다는 최근의 여러 연구 결과를 상기해보면, 본 연구 결과는 해저 지하수가 연안 해수의 pH에 미치는 영향이 매우 크다는 사실을 유추해 볼 수 있다. 따라서 해저 지하수는 연안 해수의 산성화, 저산소화 및 부 영양화와 같은 생지화학적 변화에도 큰 영향을 미칠 수 있음을 의미한다.

연안 지하수의 pH와 이와 연관된 물질 이동(예, 영양염, 유기물, 및 무기탄소의 연안 유입)은 해양 산성화에 매우 취약한 화산섬 연안 지역의 생태계와 생지화학에 커다란 영향을 미칠 수 있다. 따라서, 본 연구에서 밝힌 결과들은 연안 해수의 유출이 다른 연안 환경에서는 어떤 영향을 주는지, 또한 장기적으로는 어떻게 해양 산성화에 반응하는지에 관한 연구에 중요한 시작점이 될 것으로 기대한다.

주요어: 연안 지하수(해저 지하수), 해저 하구, 연안수의 pH, 양성자 흡착 반응, 영양염, 화산섬, 해양 산성화

학번: 2004-30946